UNIVERSITY OF TWENTE.

Rijnstate

Non-invasive continuous cardiac output monitoring using transthoracic echocardiography (TTE) in ICU patients (ACOUSTICS)

A feasibility study

J.G.A. den Duijn

Technical Medicine
M3 Master Thesis
13 September 2022

Graduation Committee:
Prof.dr.ir. C.L. de Korte
Dr. M.J. Blans
Drs. R.J. Lionarons
Drs. N.S. Cramer Bornemann
M.M.L.H. Verhulst,MSc

Preface

One year ago, almost to the day, I started this project. Now, it is over, I have completed my thesis and can look back with pride and joy on the last year. It has been an incredible year in which I got to do and learn so many things. I have taken the research itself as far as I could get it and I gave it my all. From the moment I first heard about this project two years ago I was intrigued from the start. Back then, I did not know if the idea of non-invasive and continuous cardiac output monitoring with TTE was even possible, but I was eager to prove it. And, now we have a working method that we were able to test on patients. Without the help of many people, this would not have been possible and therefore I want to thank them.

First of all, Michiel, I would like to thank you for your passion and your undying enthusiasm. From the moment we met, your passion for this project has been like an engine. You and your enthusiasm kept me going when I was not even sure it would work out. I want to thank you for all the things I got to learn from you, both clinically and academically. Finally, I want to thank you for your humour and optimism, because they made working with you not just a great opportunity, but also a great pleasure.

Marlous, I want to thank you for your guidance. Every time I was stuck in tunnel vision I could always talk with you and get a bit of an extended perspective. Also, I wanna thank you for all the times I just got to unload with you.

Chris, I want to thank you for your supervision. You were always a critical thinker, which pushed me to do things better. Your birds-eye perspective always helped me to see the bigger picture and for all of that, I want to thank you.

Nicole, thank you for your honesty, as you always told me the truth. For two years I had to pleasure of having you as my supervisor, in those years I learned a lot about myself and you were always there when I needed it. Again, I am thankful for all the things I learned from you.

Iris, I want to thank you for all your help. You not only helped with the practical things, like executing measurements or proofreading this thesis. But, you also helped me in general with my daily struggles. Working with you has been nothing but a joy.

Everybody at the Rijnstate Hospital who helped me realize this project. In particular I want to thank all intensivists: Aart, Allard, Brigitte, Dominique, Evelien, Henk, Jan, Maaike, Mark and Pauline. As well as, all the residents: Deniz, Jelle, Lassima, Mike, Roel, Roos and Thijs.

Finally, I want to thank all my friends and family. They all supported me during this year and without them, this thesis would simply not be completed. My love and gratitude to them are huge.

Abstract

Introduction: Patients admitted to the intensive care unit (ICU) are often hemodynamically unstable or at risk of becoming unstable. Sometimes more advanced hemodynamic monitoring is needed, for example the measurement of the cardiac output (CO). This is mostly done with gold standard techniques as the pulmonary artery catheter (PAC), or the Pulse index Contour Cardiac Output (PiCCO). However, these techniques only measure the CO intermittently, and are invasive to the patient. A non-invasive technique to measure the CO is transthoracic echocardiography (TTE). However, TTE cannot measure the CO continuously as opposed to the current gold standards. As the current methods are not capable of measuring the CO non-invasively and continuously, the need remains for a method that can do both. Based on these limitations a continuous CO (cCO) monitoring system using TTE was developed using an external ultrasound probe holder.
Objective: The goal of this research is to evaluate the feasibility and validity of the cCO measurements in ICU patients in addition to standard CO measurements.
Method: In this prospective observational study 15 healthy volunteers (HVs) and 18 ICU patients (IPs) were included. Each subject was measured once with the cCO method. The cCO method consists of 4 measurements: a manual CO measurement, a static cCO measurement, a second manual CO measurement and a dynamic CO measurement by performing a passive leg raise. The data were analysed for feasibility, validity, and differences between groups. The feasibility was evaluated using percentage of successful measurements.
Results: Feasibility for the cCO method was 100% for static and 73% for dynamic cCO measurements for the HVs group. Feasibility was 88% for static and 50% for dynamic cCO measurements for IPs. Mean cCO was not significantly different between static and dynamic measurements in the HV group ($t(10)=0.544$, $p=0.599$) and in the IP group ($z(9)=0.344$, $p=0.731$). No significant difference was found for the static cCO measurements between the HVs and the IP ($p=0.65$), nor for the dynamic measurements ($p=0.463$). The mean difference between manual and automatic CO was -1.1 l/min (with limits of agreements (LOA), being -0.15 and -2.1 l/min) for the HV group and -1.4 l/min (with LOA 0.13 and 3.0 l/min) for the IP group. Mean difference between automatic and PiCCO was -3.5 l/min (with LOA at -8.6 and 5.1 l/min). Mean difference between manual and PiCCO was -1.9 l/min (with LOA at -5.5 and 1.6 l/min). A significant correlation between manual and automatic CO measurements was found in HVs ($r(30)=0.776$, $p<0.001$) and in IPs ($r(32)=0.87$, $p<0.001$). No significant correlation was found between automatic and PiCCO ($r(14)=0.26$, $p=0.36$), and between manual and PiCCO ($r(14)=0.41$, $p=0.14$).
Conclusion: The cCO method is a feasible method for 100% of HVs and 88% of IPs. Measured values with the cCO method correspond strongly with manual CO and weakly correspond with PiCCO. Furthermore, no significant differences were found between healthy volunteers and ICU patients. However, further research is needed to increase sample size and further develop the cCO method.

Keywords: Cardiac Output, Continuous, Transthoracic Echocardiography, External Fixator, Intensive Care Patient

Contents

List of Abbreviations

Abbreviation	Meaning
A5C	Apical 5-Chamber
AI	Artificial Intelligence
BMI	Body Mass Index
BSA	Body Surface Area
CO	Cardiac Output
cCO	Continuous Cardiac Output
CSA	Cross-sectional Area
CVP	Central Venous Pressure
DS	Doppler Signal
ECG	Electrocardiogram
EDV	End-Diastolic Volume
HR	Heart Rate
HV	Healthy Volunteer
ICU	Intensive Care Unit
IP	ICU Patient
IPnp	ICU patient without PiCCO
IPp	ICU patient with PiCCO
IQR	Interquartile Range
LVOT	Left Ventricular Outflow Tract
LVOTd	LVOT Diameter
MAP	Mean Arterial Pressure
METC	Medical Ethical Assessment Committee
PAC	Pulmonary Artery Catheter
PAP	Pulmonary Artery Pressure
PAOP	Pulmonary Artery Occlusion Pressure
PCA	Pulse Contour Analysis
PLA	Parasternal Long Axis
PLR	Passive Leg Raise
PiCCO	Pulse index Contour Cardiac Output
PWD	Pulsed Wave Doppler
RAP	Right Atrium Pressure
SD	Standard Deviation
SV	Stroke Volume
SvO2	Mixed Venous Oxygen Saturation
TPTD	Transpulmonary Thermodilution
TTE	Transthoracic Echocardiography
VTI	Velocity Time Integral

1 Introduction

1.1 General Introduction

Patients admitted to the intensive care unit (ICU) are often hemodynamically unstable or at risk of becoming unstable [1]. Hemodynamic instability is generally caused by hypovolemia, myocardial dysfunction, and/or alterations in vasomotor function [2]. Hemodynamic instability can lead to a mismatch between oxygen delivery and demand in the tissue and can contribute to organ failure [1]. Therefore, most ICU patients need hemodynamic monitoring, consisting of electrocardiography (ECG), pulse oximetry, and monitoring of arterial pressure and temperature [1, 3]. Sometimes more advanced hemodynamic monitoring is needed, for example the measurement of the cardiac output (CO).

In approximately twelve percent of all ICU patients, primarily shock, septic and trauma patients, the CO has to be monitored [4, 5]. The CO quantifies the volume of blood pumped through the body by the heart per minute [6]. CO is a dynamic parameter and therefore constantly changing. Changes in CO can be used to guide fluid resuscitation, and administration of vasopressors and inotropic agents. For many years, the gold standard for measuring the CO was the pulmonary artery catheter (PAC), which estimated the CO invasively by measuring blood flow and pressure. It thereby allowed for constant measurement of the CO. However, it is an invasive method with significant draw backs [7]. Nowadays, the FloTrac ® and Pulse index Contour Cardiac Output ® (PiCCO) systems are less invasive substitutes for the PAC that estimate the CO using thermodilution to obtain continuous measurements. However, thermodilution techniques only measure the CO intermittently, and still requires a catheter to be inserted into the bloodstream. [2]

A non-invasive technique to measure the CO is transthoracic echocardiography (TTE). TTE can be used to obtain ultrasound images of the heart and enables the calculation of the CO. The CO can be calculated, by estimating stroke volume (SV) using TTE and multiplying it with the heart rate (HR), as seen in Formula 1. The SV is estimated by measuring the diameter of the aorta and the velocity time integral (VTI) through the left ventricular outflow tract (LVOT) using pulsed wave Doppler (PWD). When the LVOT VTI is traced on the monitor, the ultrasound machine calculates the SV. The HR is measured simultaneously using an ECG. The advantages of TTE are that it is non-invasive, quick, safe, and can be executed at the bedside. A disadvantage of TTE is that it cannot measure the CO continuously as opposed to the PAC nor intermittently as the PiCCO/FloTrac. [8]

$$CO = HR * SV \tag{1}$$

with,
CO = Cardiac Output
HR = Heart Rate
SV = Stroke Volume

As the current methods are not capable of measuring the CO both non-invasively and continuously, the need remains for a method that can. TTE appears to be the most promising method of the current techniques as it is non-invasive. Two challenges remain to be able to measure continuously: first, the probe needs to be hold in place for a longer period of time, and second, the VTI has to be automatically selected and the CO calculated from the ultrasound images. The first challenge may

be solved by using an ultrasound probe holder, for example the ProbeFix (Usono B.V., Eindhoven, Netherlands), that uses non-traumatic straps to secure the probe to the thorax for a longer period. A recent study already investigated the feasibility of the ProbeFix in ten ICU patients and demonstrated that accurate CO measurements in 80 percent of ICU patients were obtained [9]. A solution for the second challenge was investigated by another study. Their automatic calculation of CO by obtaining an apical five-chamber view of the heart using TTE had a success rate of 60 percent [10]. With artificial intelligence (AI), the pulsed wave Doppler image was optimised and four seconds of the Doppler spectrum were recorded. The algorithm then automatically traced the outline of the VTI, averaged the VTIs, and calculated the HR and CO.

Based on these recent studies, we developed a continuous CO (cCO) monitoring system using TTE in combination with the ProbeFix and automatic VTI calculation. [11, 12] Recent research at the Rijnstate Hospital in Arnhem has shown that the CO can be measured continuously in five healthy volunteers using TTE [13]. Thereby, allowing for both non-invasive and continuous CO measurements. To our knowledge there are no other studies on the use of TTE for continuous CO measurements to this date. We expect that it is feasible to use the cCO method in ICU patients, as the ProbeFix has already been tested in ICU patients as well as the cCO method in five healthy volunteers. Therefore, the goal of this research is to evaluate the feasibility and validity of these cCO measurements in ICU patients in addition to standard CO measurements

1.2 Research Objectives

The primary aim of this research is to evaluate the feasibility of cCO measurements using TTE in ICU patients. Secondary aims of this research are:

1. To evaluate the validity of cCO measurements using TTE by comparing these with manually measured CO in healthy volunteers and ICU patients;
2. To evaluate the validity of cCO measurements using TTE by comparing these with cCO measurements using PiCCO in ICU patients;
3. To investigate the differences in cCO measurements using TTE between healthy volunteers and ICU patients in terms of mean CO and variation of CO over time.

2 Background

In this section background information will be given about the regulation of cardiac output by the body, the different methods that are used to monitor the hemodynamic state and finally about sepsis, the most frequent pathophysiology requiring hemodynamic monitoring.

2.1 Regulation of Cardiac Output

Cardiac output (CO) is the defined as the amount of blood pumped by the heart per minute [6]. It is the mechanism that allows blood to flow around the body and thereby providing flow to the organs. The CO is dependent of the oxygen demand of the body and can be altered by modulating HR and SV. The regulation of the CO is a complex mechanism that involves the autonomic nervous system and both endocrine and paracrine signaling pathways. CO is generally between 5 and 6 l/min. [6]

The CO is the product of the HR and the SV, as stated in Equation 1. The HR is defined as the number of times the heart beats per minute and the SV is defined as the volume of blood ejected during each ventricular contraction. Both HR and SV can be simultaneously affected by several factors. More specific, the SV is directly affected by the arterial compliance, arterial pressure and vasoconstriction, as these affect the blood volume that leaves the heart. Furthermore, the blood volume is also affected by the venous return, which is regulated by the central venous pressure (CVP) and therefore by venoconstriction. [6]

The HR can affect the CO in a straight forward way, namely if the heart beats faster, more blood can be pumped through the heart in a period of time. If the HR is too slow, because of a bradyarrythmia, than the CO might be impaired. However, when the HR is too fast, for example by a ventricular tachycardia, this may also cause a low cardiac output, as the heart is working above its optimal speed. [14]

SV is determined by three factors, these are preload, contractility and afterload. Preload is defined as the volume at which the heart is most filled with blood at the end of diastole; this value is equal to end diastolic volume (EDV) [15]. Preload is the amount of myocardial distension prior to the systole. The force of the contraction during systole depends on the length they are stretched. An increase in distension, will result in a greater force of contraction and thereby an increase in CO. The amount of distortion is depending on the amount of ventricular filling. The contractility is the defined as the force of myocyte contraction [6]. The contractility positively affects the CO. The afterload is defined as the pressure the left ventricle must overcome to eject blood into the aorta during systole [15]. The afterload is largely dependent of the arterial blood pressure and the vascular tone. Unlike preload and contractility, the afterload is inversely proportional related to SV, therefore by reducing afterload, the SV increases. [6, 14]

Often the Frank-Starling curve is used to express the dynamics of CO, which can be seen in Figure 1. The Frank-Starling relation relates the preload, expressed as left ventricular EDV (or right atrial pressure), to cardiac performance, measured as cardiac output (or venous return). In this relation the CO increases when the EDV increases. The Frank-Starling curve is based on the link between the length of myocardial fibers and the force generated during contraction. There is an optimal length between the fibers at which the tension is greatest, resulting in the greatest force of contraction. The greater the EDV the more the fibers are stretched during the diastole. If the fibers are stretched further than the optimal length, the CO will not increase. When contractility is increased, for example due to nor-epinephrine infusion, the cardiac output increases for a given

preload. Graphically, resulting as an upward shift of the curve. When afterload changes, this can also be seen in the Frank-Starling curve. A decrease in afterload, will result in an upward shift of the curve, as the afterload is inversely correlated to the cardiac performance. [16]

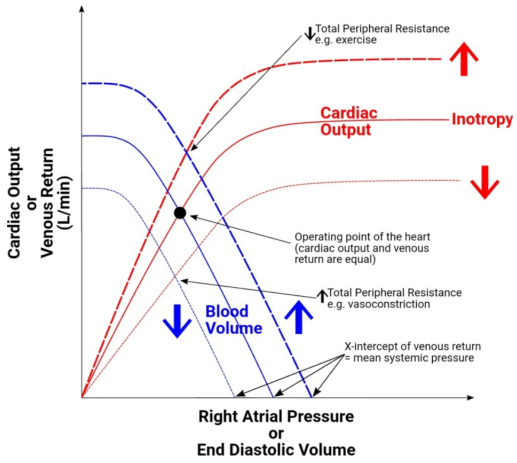

Figure 1: Frank-Starling Curve [16]

2.2 Hemodynamic Monitoring

There are different methods to monitor a patient's hemodynamic state. In this section the ones relevant to this research will be discussed, being the PAC, the PiCCO and TTE.

2.2.1 Pulmonary Artery Catheter

The pulmonary artery catheter (PAC) or also known as the Swan-Ganz catheter is a flow-directed catheter, that is placed the in pulmonary artery. The PAC is seen as the gold standard for cardiac output monitoring. The PAC is used as a monitoring equipment that simultaneously monitors three types of parameters, being cardiac output, mixed venous oxygen saturation (SvO2) and intravascular pressures. [2, 17]

The PAC calculates the cardiac output by using the thermodilution technique. In thermodilution a change in temperature is measured after the injection of a cold fluid with a given volume. Usually, a 10 ml bolus of cold saline is used. A thermistor attached to the PAC then measures the change in temperature in the pulmonary artery. This is then repeated and a mean value is computed. Using the Stewart-Hamilton equation, which can be seen in Equation 2, the CO can be calculated based on the change in temperature by the cold injection. [18]

$$CO = \frac{(T_B - T_I) * V_I * K}{\int \Delta T_B dt} \tag{2}$$

with, T_B = blood temperature
T_I = Injectate temperature
V_I = Injectate volume
K = Correction constant
$\int \Delta T_B dt$ = Area under the thermodilution curve

Beside from cardiac output measurements the PAC also allows for assessment of oxygenation by

assessing the SvO2. This can be done by taking a blood sample from the PAC. More modern PACs are equipped with fiberoptic fibers, allowing for continuous measurements. If the SvO2 is low and the arterial blood has sufficient oxygenation, this can indicate an inadequate cardiac output. The SvO2 can therefore be used as an additional parameter to assess the cardiac output. Finally, the PAC also measures intravascular pressures, more specific the pulmonary artery pressure (PAP), the right atrial pressure (RAP) and pulmonary artery occlusion pressure (PAOP) (also known as the wedge pressure). These pressures can indirectly give an indication about the cardiac output. As the PAP represents the right ventricular afterload. Furthermore, the RAP can be equaled to the CVP, which gives a value for the preload. Finally, the PAOP gives an indication for the left arterial pressure, which is a value for the filling pressure in the left atrium. [2, 17]

The PAC is positioned by placing the catheter in a vein, most commonly the jugular or the subclavian vein. It is then moved through the right atrium and the right ventricle till the catheter tip is positioned in the pulmonary artery. A balloon is then inflated to keep the PAC in position. This procedure is associated with several complications, due to the invasive nature of the procedure. Examples including pneumothorax, infection, arrhythmia's and damage to heart valves and/or myocardial tissue. [17]

The PAC has the benefit that it allows for continuous hemodynamic monitoring. But besides the downsides associated with the placement procedure, a clear survival benefit is not proven [19]. Furthermore the PAC is associated with a large inter-observer variability, which often lead to misinterpretation of data. Therefore, the PAC is less used these days and more modern monitoring devices are used, such as the PiCCO. However, the PAC remains valid for patients with pulmonary hypertension or right ventricular heart failure, as the PAC is the only device that measures the pressures in the right heart and pulmonary system. [2, 20]

2.2.2 Pulse index Continuous Cardiac Output

The Pulse index Continuous Cardiac Output (PiCCO) is a hemodynamic monitoring system. It applies an algorithm that combines real-time continuous monitoring based on pulse contour analysis (PCA) with intermittent transpulmonary thermodilution (TPTD) measurements in order to calculate CO, based on Formula 3. PCA is a technique in which SV is based on pulse pressure. The pulse pressure is measured using an arterial line to which a blood flow sensor is connected. The PiCCO uses the TPTD technique as an external calibration for the PCA. TPTD is similar to thermodilution used in PAC. However the bolus of injectate passes the complete heart and lungs, before the change in temperature is measured with the thermistor tip in the arterial line. It is recommended to re-calibrate once every eight hours. For PiCCO two lines have to be placed one arterial line, which is typically placed in the femoral artery and one central line, typically placed in the jugular or subclavian vein. [21, 22]

$$CO = cal * HR * \int_{systole} (\frac{P(t)}{SVR} + C(p) * \frac{dP}{dt})dt \tag{3}$$

with,
cal = calibration factor
HR = heart rate
$systole$ = systolic portion of the curve
$P(t)$ = pressure change over time

SVR= systemic vascular resistant
$P(t)/SVR$ = the are under the arterial pressure curve in systole
$C(p)$ = aortic compliance
dP/dt = shape of the arterial waveform

The PiCCO system has several advantages, mainly that by using the TPTD as calibration it validates the CO measurements and thereby has an accuracy that is comparable with the PAC. Furthermore, it combines TPTD with PCA, which allows for a continuous display of CO. Finally it gives insight in other useful parameters, including stroke volume variation, global end-diastolic volume and extravascular lung water. However there are also several disadvantages to the PiCCO. Firstly, the requirement of both an intra-arterial and central venous access, Secondly the inability to measure pulmonary artery pressures. And, finally the unreliability of PCA in patients with arrhythmia's, aortic valve pathology and mechanical circulatory assist devices. [22]

2.2.3 Transthoracic Echocardiography

Transthoracic echocardiography (TTE) is an imaging modality that is used to assess cardiac performance. The CO can also be calculated using TTE. With TTE the SV is obtained from the product of the LVOT cross-sectional area (CSA) and the LVOT VTI, as seen in Equation 4. The LVOT CSA is derived from the LVOT diameter (LVOTd), by using the standard formula for the area of a circle, as seen in Equation 5. The LVOTd is measured from the parasternal long axis (PLA) view. The LVOTd corresponds to the diameter of the annulus of the aorta [23]. The LVOT VTI is determined by using the PWD mode on an apical five-chamber (A5C) view of the heart. The LVOT VTI is then traced to calculate SV and CO. An example can be seen in Figure 2 [24]

$$SV = LVOT_{\text{CSA}} * LVOT_{\text{VTI}} \tag{4}$$

$$LVOT_{\text{CSA}} = (LVOT_{\text{d}})^2 * \pi \tag{5}$$

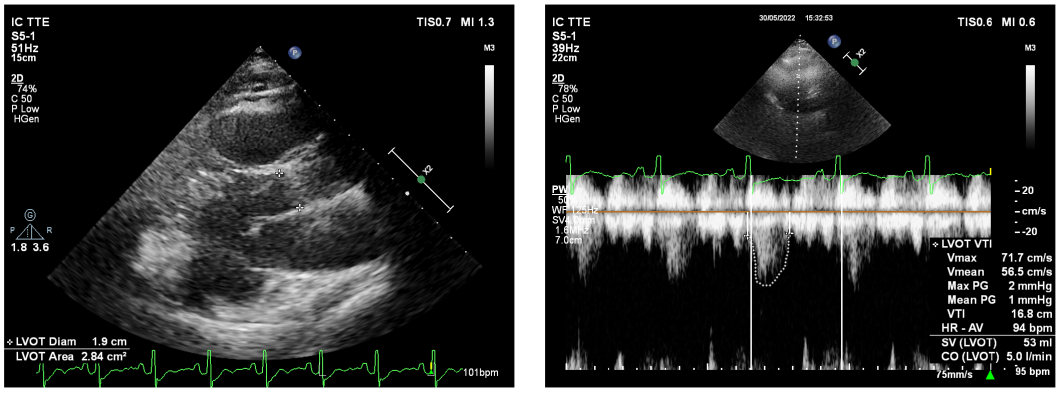

Figure 2: Example of a manual CO measurement using TTE

TTE has several advantages. Most important, being that is non-invasive for patients. Furthermore it is cheap, usable at bedside, easily repeatable, extensively available and does not use ionizing radiation. Furthermore, TTE offers the ability to link CO status to its causative factor, for example cardiac dysfunction, hypovolemia or tamponade. Disadvantages to TTE are the inability to continuous monitoring and the many manual steps to perform CO measurements. [24]

2.3 Sepsis

Sepsis is defined as life-threatening organ dysfunction caused by a dysregulated host response to an infection [25]. The exact pathophysiology is complex and not fully understood, although it has been linked to several cellular mediators. The release of multiple inflammatory mediators during sepsis leads to multi-organ failure, therefore it is managed as a systemic disorder. Symptoms can include, hypoxia, tachypnea, altered mental status, hypotension and acute kidney injury. Early recognition of sepsis is key and there symptoms are tracked using the quick Sepsis-related Organ Failure Assessment. If patients are suspected of having sepsis, early treatment is recommended. Treatment includes, source control using antibiotics and a combination of fluid resuscitation and vasopressor to avoid hypotension. Sometimes sepsis develops into septic shock. Septic shock is defined as a subset of sepsis in which underlying circulatory and cellular/metabolic abnormalities are profound enough to increase mortality substantially [25]. Clinical septic shock is identified as persistent hypotension, requiring vasopressors to keep a mean arterial pressure (MAP) above 65 mmHg and an elevated serum lactate above 2 mmol/L, despite adequate fluid resuscitation. [26, 27]

Oxygen transport and delivery are key in treatment of sepsis and septic shock. This is best monitored by using CO as a parameter, because CO directly reflects the state of the cardiovascular system. Because CO is not regulated by neuro-humoral reflexes as opposed to blood pressure, it may suddenly drop before the development of hypotension. Also, the CO can easily be used to track therapeutic effect of treatment. Variations in CO can easily be tracked by several techniques. Measurement in CO provides valuable information on the stability of the hemodynamic status of the patient and/or the development of significant abnormalities within the cardiovascular system. Therefore it plays a key part in sepsis treatment. [5]

3 Methods

3.1 Study Design

This prospective observational study was approved by the Medical Ethics Assessment Committee (METC) Nijmegen (2021-13413) and by the local hospital board Rijnstate (2021-1997). Data collection was performed between March and June 2022 at the ICU department of the Rijnstate Hospital, Arnhem, The Netherlands. The study consisted of two phases: the feasibility phase, in which the study procedure and measurement setup were tested on healthy volunteers (HV), and the testing phase, in which the cCO method was tested and validated on ICU patients (IPs).

3.2 Study Population

Subjects were classified in one of three study groups: Healthy Volunteers (HVs), IPs without PiCCO (IPnp) or IPs with PiCCO (IPp). HVs were selected among the staff of the ICU department. All patients admitted to the ICU department of the Rijnstate Hospital in Arnhem were screened for potential participation.

Inclusion criteria for all subjects were an age older than 18, having a body mass index (BMI) $<$40 kg/m^2. Further inclusion criteria for IPs were admission to the ICU, sinus rhythm and an indication for hemodynamic monitoring. The indication for hemodynamic monitoring, could either be receiving noradrenaline or having a MAP below 65 mmHg and/or the professional opinion of an intensivist. For the IPp group the final inclusion criteria was hemodynamic monitoring with a PiCCO catheter. Exclusion criteria were pregnancy and/or traumatic injury to the thorax.

If subjects were awake and competent, written informed consent was signed by the subject. If patients were not awake or competent, a legal representative signed informed consent. If patients regained consciousness afterwards, they were also asked for signed informed consent.

3.3 Study procedure

All subjects were measured using the cCO method. This method consists of four measurements: two manual CO measurements, one static cCO measurement with the ProbeFix, where the patient is laying down, and one dynamic cCO measurement in which a passive leg raise (PLR) is performed. During the PLR the legs of the patient are moved in a 45 degree angle by tilting the bed, as seen in Figure 3. The cCO method takes 15 minutes, each subject was measured once. Before the measurements started descriptive variables (sex, age, length, weight, and medication use) were collected. Reason of admittance was also noted.

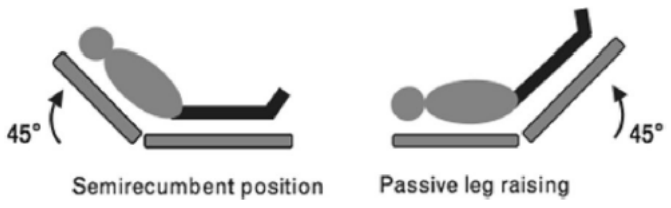

Figure 3: The two positions in PLR.[9]

Ultrasound recordings were made with the Affinity 70c ultrasound system (Philips, Eindhoven, Nether- lands), using a PureWave S5-1 transducer (Philips, Eindhoven, Netherlands) and the Aquasonic 100 ultrasound gel (Parker Laboratories Inc., Fairfield, NJ, USA). Subjects were first scanned

with the ultrasound in the PLA view to measure the LVOT diameter. Next, an A5C view was made in order to establish if an adequate PWD signal could be generated. If a clear A5C view was obtained, the ultrasound was then fixated to the thorax by placing the ultrasound probe into the ProbeFix (Usono, Eindhoven, Netherlands) ultrasound holder. Additionally, three 24 mm, Ag/AgCl ECG electrodes (Kendall, Covidien, Medtronic Inc., Minneapolis, MN, United States), were placed, two on either side of the thorax just below the clavicle and one on the right side of the lower abdomen to measure the ECG. These were then connected to the ultrasound system using a 3-lead ECG cable Grabber IEC (Philips, Eindhoven, Netherlands). If a subject was attached to the IntelliVUe MX800 monitoring system (Philips, Eindhoven, Netherlands), a NYS201 double-sided AUX cable (Rean, Neutrik Group, Schaan, Liechtenstein) would be used to connect the ultrasound system with the monitoring system. This allowed for a real-time ECG signal on the screen of the ultrasound, that could be simultaneously recorded with the ultrasound images. An overview of the measurement setup can be seen in Figure 4.

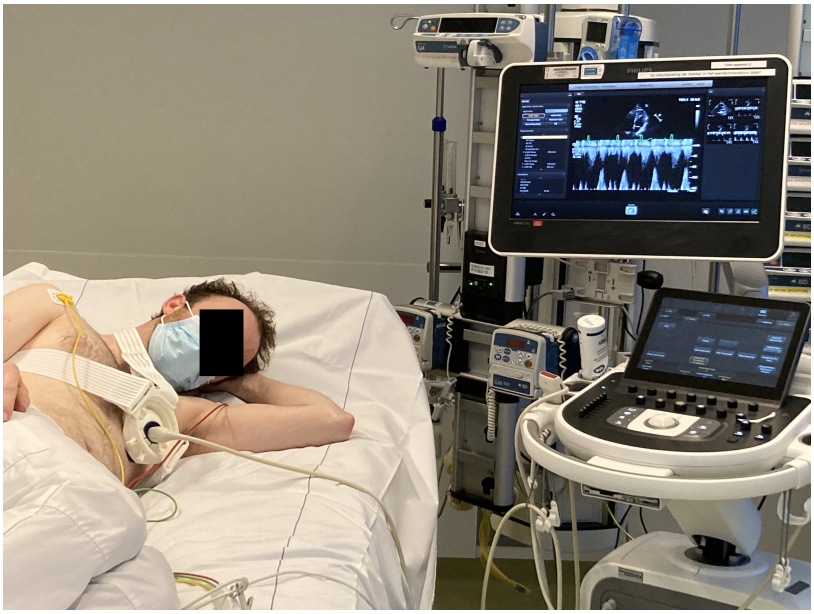

Figure 4: Overview of measurement setup

As stated before the cCO method consists of 4 measurements. For each measurement the PWD mode was activated, a solid image was established and the baseline was centered on the screen of the ultrasound. By centering the baseline the complete VTI signal could be displayed over the length of the screen, which was needed for the analysis. For the first manual CO measurement the loop time was set to three seconds. The VTI was recorded and traced, the HR was calculated from the ECG signal and the CO was manually calculated. For the IPp group the CO value measured by the PiCCO was noted from the monitoring system simultaneously. For the static measurement the loop time was set to three minutes and subjects were instructed to lay still. For the second manual measurement, loop time was set back to three seconds and the same steps were followed as for the first manual CO measurement. Finally, for the dynamic cCO measurement, loop time was set to five minutes, and patients were instructed about the PLR. After one minute a PLR was performed, and at three minutes the bed was placed back in normal position. All patients were evaluated upfront whether or not they were capable of undergoing PLR. After the final measurement the ProbeFix was removed from the subjects thorax and all data was exported from the ultrasound system. An overview of the measurement protocol is shown in Figure 5.

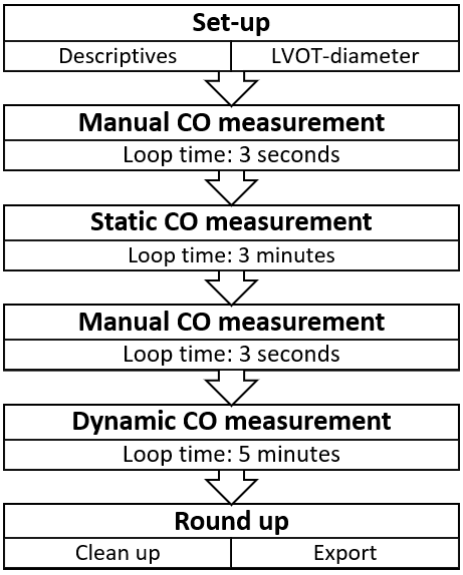

Figure 5: Overview of study procedure for cCO method

3.4 Analysis

The data were pre-processed and analysed using an algorithm created in MATLAB (version 2020b, MathWorks, Natick, MA, USA), the scripts of this algorithm are shown in Appendix A. The pre-processing steps in this algorithm are shown in Figure 6. First, the TTE image is selected from the recordings. A frame was selected in which a full-length Doppler signal (DS) was seen over the length of the frame. A full-length DS was identified as the first frame displaying the red baseline at the upper right corner of the screen. Secondly, this image is cropped, as only the DS below the baseline is of interest. The DS was cropped by using color detection on the baseline, because the baseline is the only red object on the screen. Thirdly, the cropped frame is transferred to greyscale and then binarized, converting the frame to black and white. Pixels with a luminance greater than 10 were replaced with 255 (white), all other pixels were replaced with value 0 (black). The threshold of 10 was chosen based on previous research, that showed the best binarization for a threshold of 10 [12]. Fourthly, the holes in the binarized frame were filled. The edges of the binarized frame are found and connected using the Canny edge method. The Canny edge method finds the edges by looking for the local maximum of the gradient of the image [28]. These edges are then connected by applying morphological operations such as: bridging unconnected pixels, dilating and eroding the image. Fifthly, the bridged frame was converted from the frame to a signal. This was done by selecting the white pixel with the lowest absolute velocity at every time point. Finally. the signal was scaled based on the frame rate and smoothed with a Savitzky Golay filter (25 windows), creating the final signal.

These steps were then repeated for the entire ultrasound recording. Essentially, the signal is obtained per screenshot of the recording. For example, if the complete recording existed of 10 screenshots, 10 signal segments were obtained. These segments were merged and compose the complete signal. The final step was to exclude data in the signal that was corrupted by artifacts or noise per subject by visual inspection. The signal was plotted and a first threshold was defined that removed all excessive data. Next, a second threshold for the remaining corrupted data was defined. The remaining corrupted data, in combination with 20 samples before and after the threshold, was

removed and recovered using a third order derivative filter, an example can be seen in Figure 7. Thereby, finishing the pre-processing.

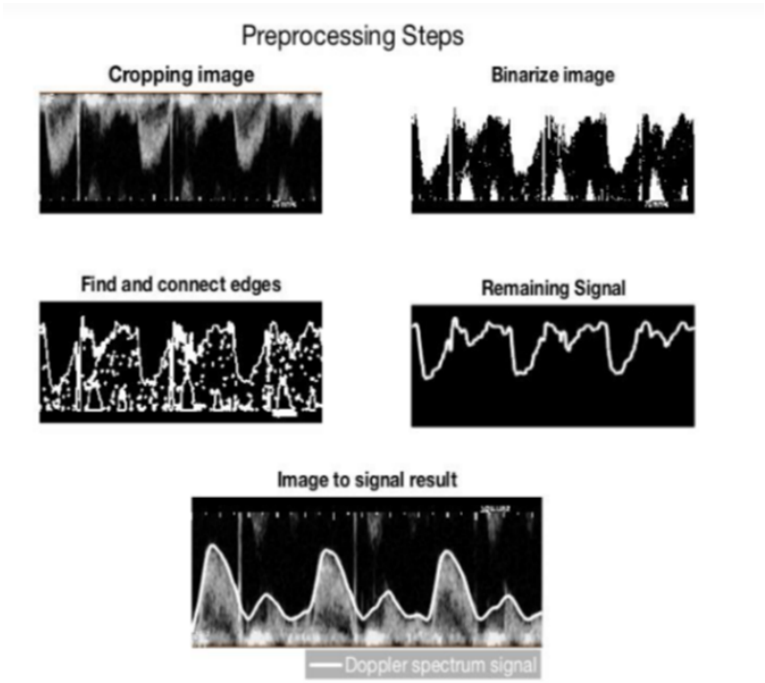

Figure 6: Overview of pre-processing steps. First the signal is cropped, followed by binarization of the image. The edges of this binarized image are identified and with the Canny edge detection method a signal remains. As final step, the signal is scaled and smoothed with a Savitzky Golay filter. In the bottom image the final signal (shown in white) is plotted over the TTE image. [13]

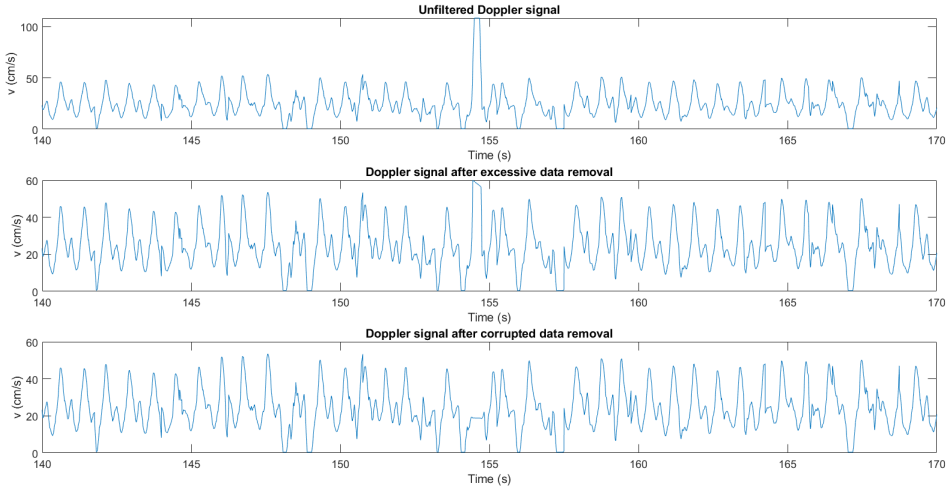

Figure 7: Overview of filtering steps of the Doppler signal

After pre-processing, the signal was used for the automatic VTI estimation, as seen in Figure 8. The LVOT VTI was defined as the area in the DS that represents the systolic flow of the LVOT. Therefore, the automatic detection needed to detect the ejection during systole. The automatic calculation of the VTI was done in four steps. Firstly, the local points of maximum velocity are detected in the DS

by using the findpeaks function in MATLAB (yellow point). Secondly, the start of the ejection was detected. It was defined as the last point where the velocity had a local minimum before it reached the local maximum. This corresponded with the start of the systole and therefore the place where manual tracing starts as well. This point was detected by looking at the acceleration of the DS and matching the zero-crossing before the maximum as the start point (red point). The acceleration of the DS is acquired by using a simple derivative of the DS. Thirdly, the end of the ejection phase had to be detected. This was defined as the local minimum after the local maximum, as this again corresponded with the manual tracing. This point was detected again by using the acceleration of the DS, but this time by looking for the zero-crossing after the local maximum (orange point). Lastly, the VTI is calculated by trapezoidal numerical integration of the DS during the ejection. This is then multiplied with the LVOTd and the SV is calculated.

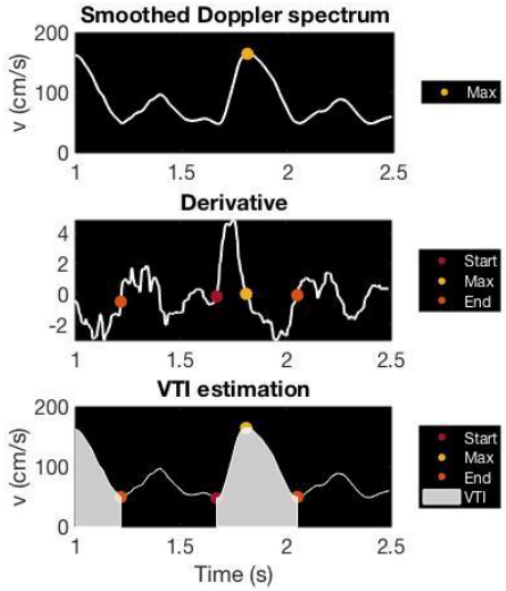

Figure 8: Example of the automatic VTI estimation. [13]

Finally, the number of heartbeats was set over which the CO was averaged. In this research a number of three heartbeats was used in the calculation of the CO. As research indicates that averaging over three heart beats is sufficient for obtaining a precise VTI in patients with sinus rhythm [8]. The CO was calculated following formula 1.

All steps of the analysis were combined in an interface for the physician, as seen in Figure 9. This interface shows the complete smoothed DS, the window of three VTIs, the acceleration with the start-, maximum- and end point for each ejection, the estimated VTI, the CO averaged for the set window as a number, and the CO as a point in the trend line.

The data were analysed for feasibility, validity and differences between groups. The feasibility was evaluated using percentage of successful static measurements, percentage of successful dynamic measurements and percentage of successful analyses. A successful measurement was defined as a measurement in which the VTIs could be measured consecutively, without a prolonged interruption of more than 15 seconds, for the duration of the measurement. A successful analysis was defined as an analysis for which at least the data of one successful measurements was provided and for which the CO could be calculated consecutively without structurally altering the data. The

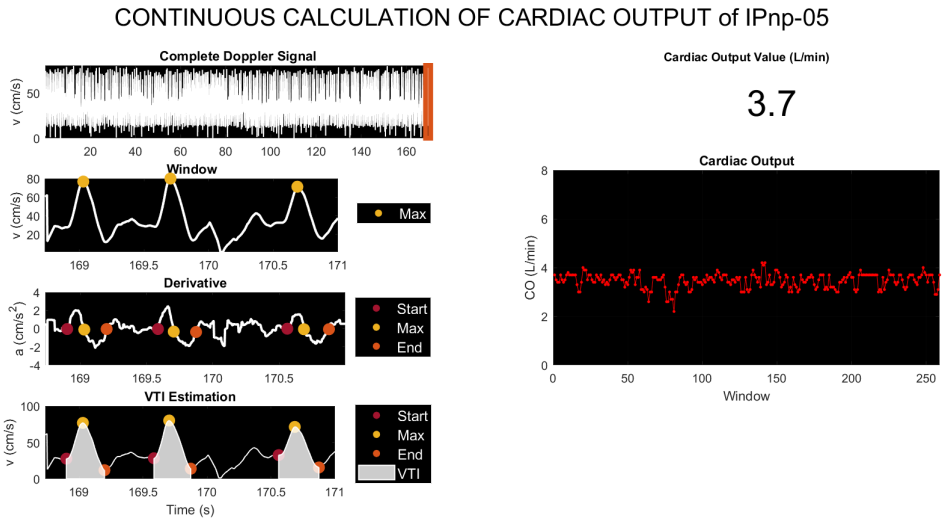

Figure 9: Example of the physician's interface for an ICU patient

validity was evaluated, using mean, median, maximum and minimum CO for both groups during static and dynamic measurements. Furthermore the validity was evaluated by comparing the automatic and manual CO values. For the IPp group the CO value determined by the PiCCO was also compared with the manual and automatic CO values.

3.4.1 Statistical Analysis

Statistical analysis was executed with SPSS (version 26, IBM Statistics, Armonk, NY, USA). Data were tested for normality using the Shapiro-Wilk test. Data were presented as mean with standard deviation (SD) when normally distributed and as median with interquartile range (IQR) when not normally distributed. Subject characteristics were tested for significant differences using either a independent t-test when normally distributed or the Mann-Whitney U test when not normally distributed. Difference between mean static and dynamic CO were tested using a paired samples t-test for HVs and the Wilcoxon signed rank test for the IPs. Correlation between manual and automatic CO was tested using Pearson correlation coefficient. Correlation was defined as strong for $r>0.7$, as moderate for $0.4<r<0.7$ and weak for $r<0.4$ [29]. Furthermore, scatter plots and Bland-Altman plots of agreement were made for manual and automatic CO calculation for the HV and IP group. Also, scatter plots and Bland-Altman plots of agreement were made for PiCCO and manual CO, and for PiCCO and automatic CO for the IPp group. Finally, difference between HV and IP group for static and dynamic measurements was tested with the Mann-Whitney U test.

4 Results

4.1 Inclusion

The inclusion process, following the study design, resulted in 15 HVs and 18 IPs. Of these 18 IPs, 8 had a PiCCO catheter. 18 potential HVs were assessed for eligibility. 2 HVs turned out to have an exclusion criteria and one declined to participate. 15 HVs were included and analysed. 51 patients were assessed for eligibility. 27 subjects did not meet the inclusion criteria, most frequently because of ongoing atrial fibrillation. 8 patients declined participation or measurements were not achievable due to logistic reasons. A total of 18 patients were included. For the analysis, 2 patients were excluded, as no clear A5C view could be achieved and therefore no data could be collected. This resulted in 16 IPs for analysis. An overview of the enrolment is shown in Figure 10.

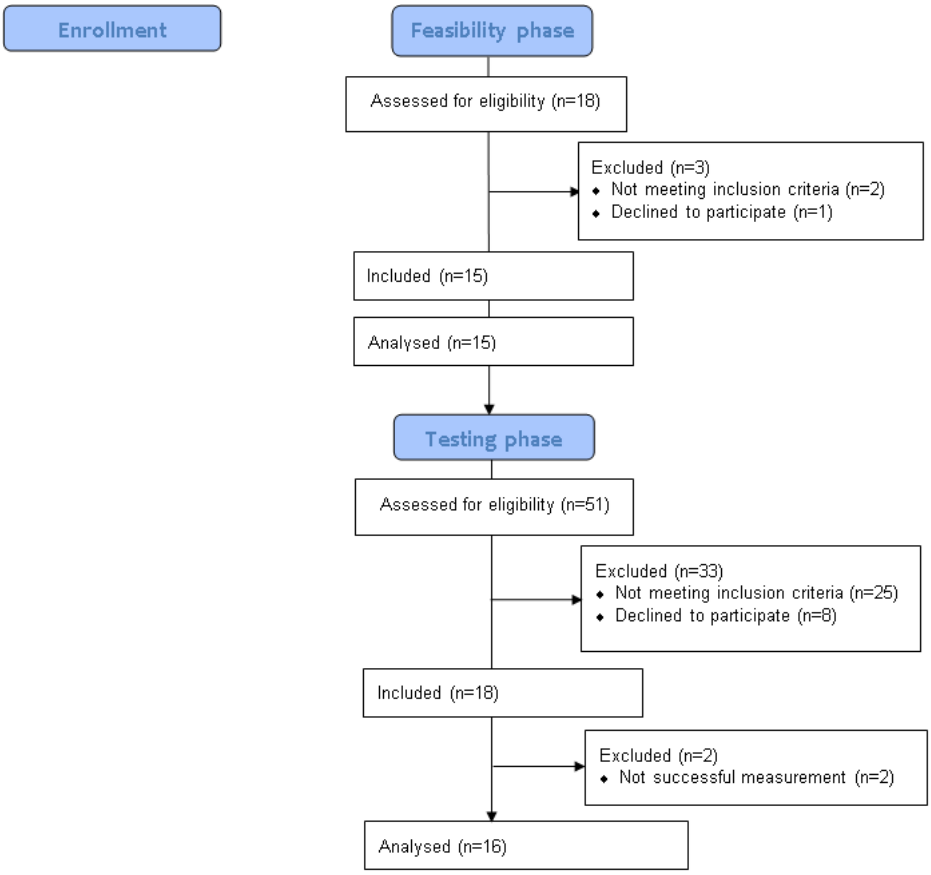

Figure 10: Flow chart for cCO study

4.2 Subject Characteristics

Subject characteristics and the corresponding p-values are shown in Table 1 for the HVs and the IPs. Data per subject is shown in Appendix B. The HVs consisted of fifteen subjects, seven males and eight females, with an average age of 27 years and an average BMI of 23.4 kg/m2. The IP group consisted of 18 people, 13 males and 5 females, with an average age of 64 years and an average BMI of 28.4 kg/m2. Zero HVs and 12 IPs used medication that have a direct effect on the CO. Both groups had an average LVOT diameter of 2.0 cm. Age, weight, BMI, body surface area (BSA) and medication use were significantly different between the HVs and IPs, all statistical output from SPSS is shown in Appendix C.

Subject characteristics and the corresponding p-values for the two IP subgroups (IPp and IPnp) are shown in Table 2. The IPp group consisted of eight subjects, five males and three females, with an average age of 64 years and a BMI of 28.9 kg/m2. In the IPp group five patients were admitted with a sepsis, one with septic shock, one for respiratory insufficiency and one for post-operative monitoring. Seven subjects in the IPp group used medication. All IPp that used medication were administered noradrenalin, four argipressin, two hydrocortisone, one enoximone, one nifedipine and one used metoprolol. The IPnp group consisted of 10 subjects, 8 males and two females, with an average age of 64 years and an average BMI of 28.0 kg/m2. Reason of admittance varied among this subgroup, as one was admitted with sepsis, two with respiratory insufficiency, two for post- operative monitoring, two after out-of-hospital cardiac arrest (OHCA), two with COVID-19 and one after trauma. Five subjects used medication in the IPnp group, four used metoprolol, two were administered noradrenalin, and one enoximone. No subject characteristics were significantly different between the two subgroups.

Characteristic	**HV (n=15)**	**IP (n=18)**	**P-value**
Gender (M/F)	7/8	13/5	0.141
Age (years)	27 (±3)	64 (±10)	$<$.001*
Length (cm)	1.77 (±0.09)	1.76 (±0.08)	0.718
Weight (kg)	73.4 (±9.3)	87.3 (±10.3)	0.007*
BMI	23.4 (±1.5)	28.4 (±4.8)	0.007*
BSA	1.9 (±0.2)	2.1 (±0.1)	0.022*
Medication use (N=)	0	12	$<$.001*
LVOT diameter (cm)	2.0 (±0.1)	2.0 (±0.1)	0.344

Table 1: Subject Characteristics

Characteristic	IPp (n=8)	IPnp (n=10)	P-value
Gender (M/F)	5/3	8/2	0.423
Age (years)	64 (±9)	64 (±11)	0.994
Length (cm)	1.76 (±0.10)	1.77 (±0.06)	0.804
Weight (kg)	87.5 (±12.6)	87.2 (±8.5)	0.592
BMI	28.9 (±6.7)	28.0 (±3.4)	0.742
BSA	2.1 (±0.1)	2.1 (±0.1)	1.00
Reason of Admittance Sepsis Shock Post-operative Respiratory insufficiency OHCA COVID-19 Trauma	 5 1 1 1 0 0 0	 1 0 2 2 2 2 1	
Medication use (N=) Noradrenalin Argipressin Hydrocortisone Metoprolol Enoximone Nifedipine	7 7 4 2 1 1 1	5 2 0 0 4 1 0	0.103
LVOT diameter (cm)	2.0 (±0.1)	2.0 (±0.1)	0.625

Table 2: Subject Characterisitics For the IP Subgroups

4.3 Feasibility

The feasibility of the cCO method was expressed as the percentage of successful static and dynamic measurements, and percentage of successful analyses. As shown in Table 3, for the HV group, the static cCO measurements were 100% successful, dynamic cCO measurements were 73% successful and analyses were also 100% successful. For the IP group, static measurements were successful in 88%, as well as 50% of dynamic cCO measurements and 100% of analyses. The two IP subgroups were also compared for feasibility. In the IPp group, 88% of static cCO measurements were successful, 38% of dynamic cCO measurements and 100% of analyses. For the IPnp, static cCO measurements were successful in 90%, dynamic cCO measurements in 60% and 100% of analyses.

	HV	IP		
		Total	IPp	IPnp
Successful static measurements (%)	100	88	88	90
Successful dynamic measurements (%)	73	50	38	60
Successful analyses (%)	100	100	100	100

Table 3: Percentage of successful static measurements, dynamic measurements and analyses for all groups

4.4 Healthy Volunteers

The average cCO per HV was normal distributed. Manual and automatic cCO data were also normally distributed. The HVs had a median cCO of 2.8 l/min for both the static and dynamic measurements, with an IQR of 1.2 and 1.3 l/min respectively. The maximum CO for the static cCO measurements was 4.0 l/min and 4.3 l/min for the dynamic cCO measurements. The minimum cCO was 1.9 l/min for both the static and dynamic measurements. Mean cCO did not differ between static and dynamic measurements in the HV group (t(10)=0.544, p=0.599).This is also shown as a box plot in Figure 11. Furthermore, a scatter plot and a Bland- Altman plot of agreement between the manual and automatic measurements for the HVs are shown in Figure 12. The mean difference between manual and automatic CO was -1.1 l/min, with limits of agreements (LOA), being -0.15 and -2.1 l/min and the reproducibility coefficient (RPC) being 0.96. Finally, a significant correlation between manual and automatic CO measurements is seen in HVs, with Pearson's r(30)=0.776 and $p<0.001$.

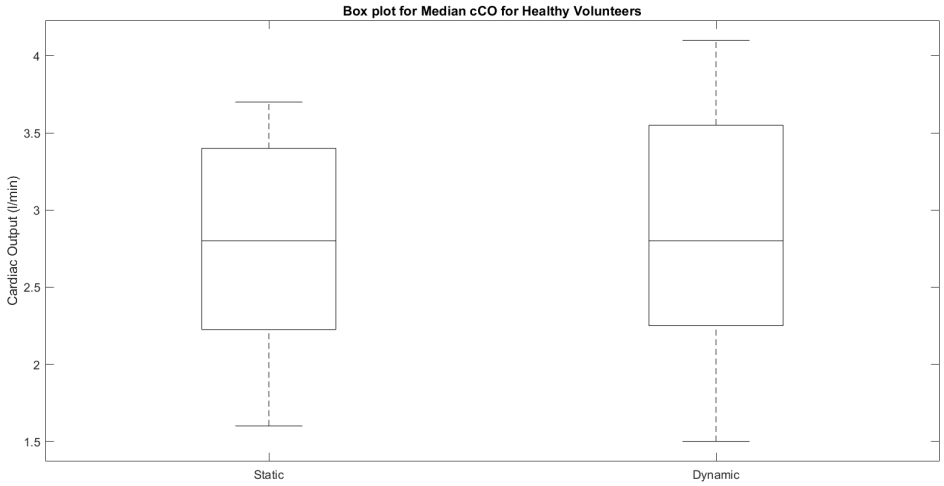

Figure 11: Box plot for median cCO for healthy volunteers (HVs)

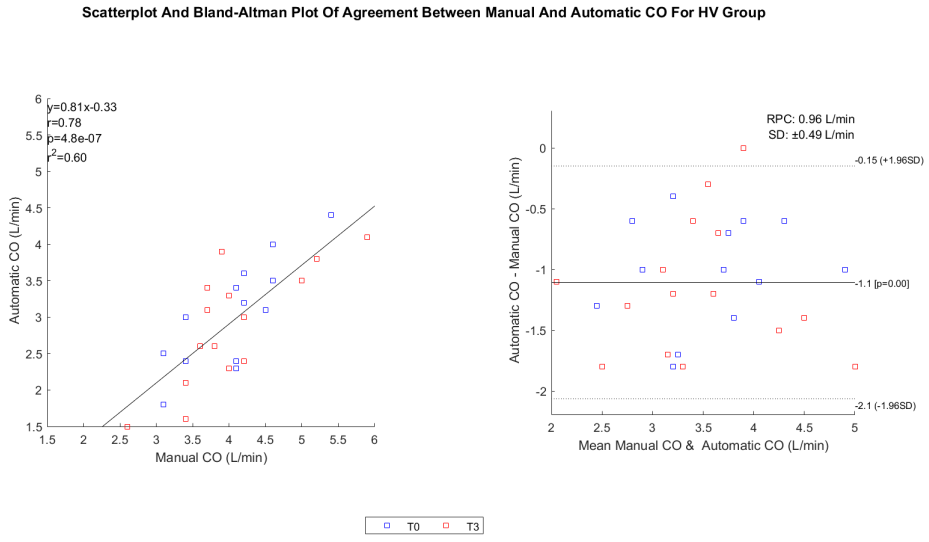

Figure 12: Scatter plot (left) and Bland-Altman plot (right) between manual and automatic CO for healthy volunteers (HVs)

4.5 ICU Patients

The average cCO per IP was not normally distributed. Manual and automatic cCO data were normally distributed. As shown in Figure 13, the static measurements had a median of 3.1 l/min with an IQR of 0.9 l/min. The dynamic CO measurements had a median of 3.2 l/min with an IQR of 1.5 l/min. Mean cCO did not differ between static and dynamic measurements in the IP group ($z(9)=0.344$, $p=0.731$). Finally, scatter plot and a Bland-Altman plot of agreement between the manual and automatic measurements are shown in Figure 14. The mean bias was -1.4 l/min, with LOA at 0.13 and 3.0 l/min and a RPC of 1.5. Furthermore, Figure 11, shows a significant correlation between manual and automatic CO measurements in ICU patients, with Pearson's $r(32)=0.87$, $p<0.001$.

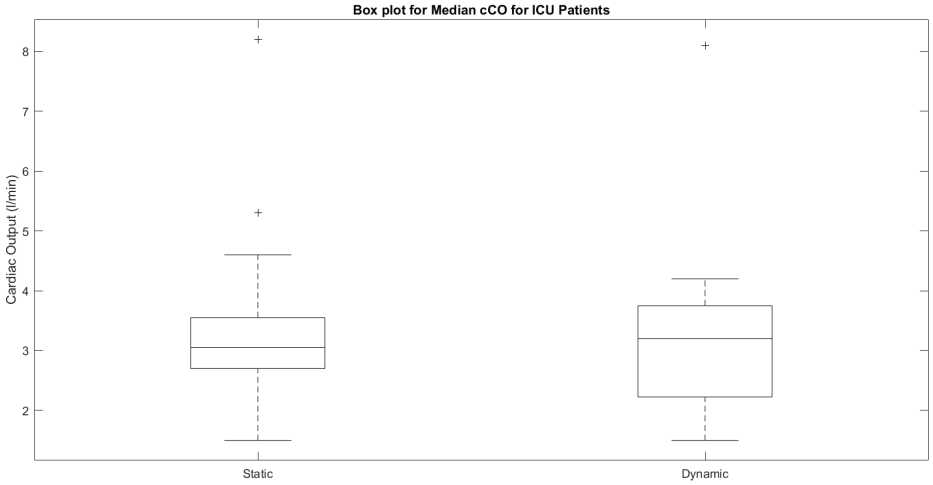

Figure 13: Box plot for median cCO for ICU patients (IPs)

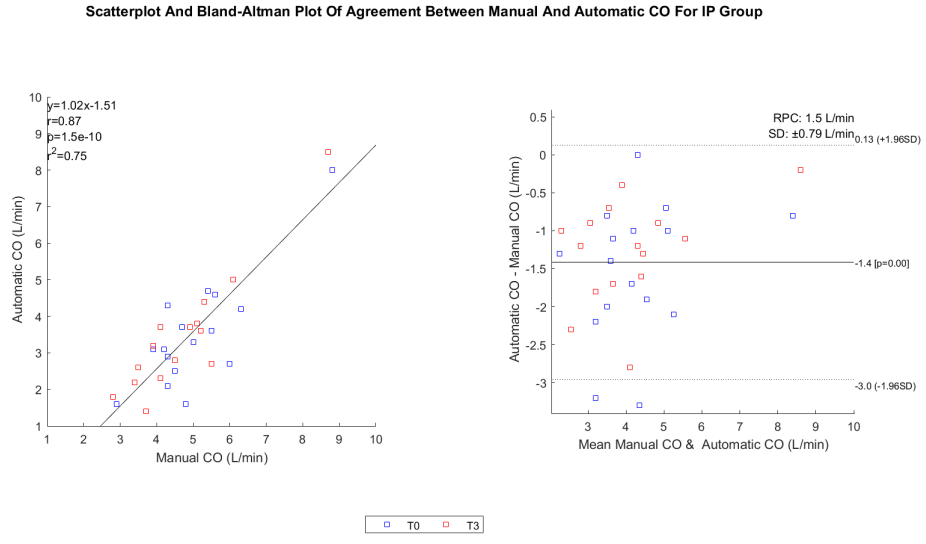

Figure 14: Scatter plot (left) and Bland-Altman plot of agreement (right) between manual and automatic CO for ICU patients (IPs)

4.5.1 ICU Patients Subgroups

A post-hoc analysis was conducted for the two ICU subgroups. A box plot is shown in Figure 15, showing the medians for both groups. The IPp group has a median of 3.1 l/min for the static cCO measurements with an IQR of 0.8 l/min. The dynamic CO measurements had a median of 3.3 l/min with an IQR of 0.5 l/min. For the IPnp group the median was 3.0 l/min for the static measurements with an IQR of 2.2 l/min and for the dynamic measurements the median was 2.0 l/min with an IQR of 2.0 l/min. Furthermore, a scatter plot and a Bland-Altman plot of agreement between the PiCCO and the automatic CO are shown in Figure 16. The mean bias was -3.5 l/min with LOA being -8.6 and 5.1 l/min and RPC at 5.1. Further, Figure 16 shows that the correlation between automatic and PiCCO CO was not significant, with Pearson's r being -0.26 with p=0.36. Finally, a scatter plot and Bland-Altman plot of agreement between the PiCCO and manual CO are shown in Figure 17. The mean bias was -1.9 with LOA being -5.5 and 1.6 l/min and RPC at 3.6. The correlation between manual and PiCCO was moderate and not significant with Pearson's r being 0.41 with p=0.14.

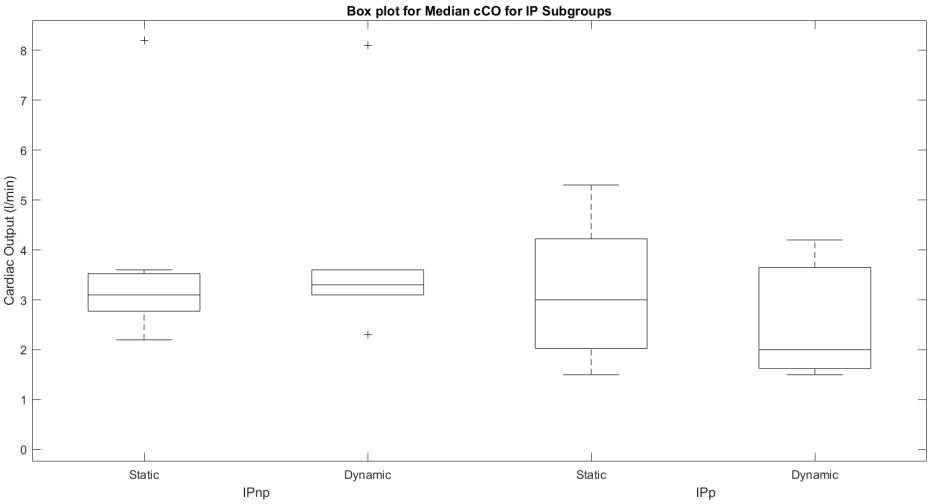

Figure 15: Box plot for median CO for the ICU patients with PiCCO (IPp) and the ICU patients without PiCCO (IPnp) groups

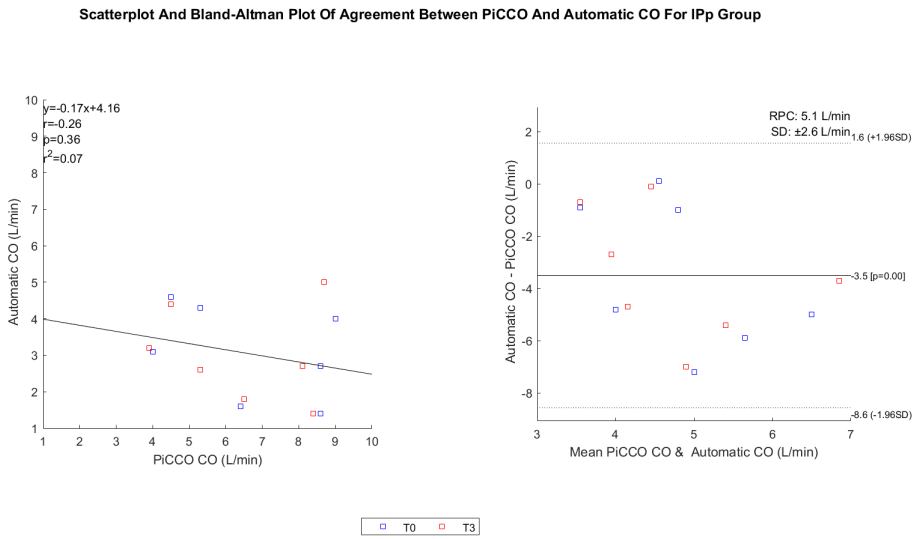

Figure 16: Scatter plot (left) and Bland-Altman plot of agreement (right) between PiCCO and automatic CO for ICU patients with PiCCO (IPp)

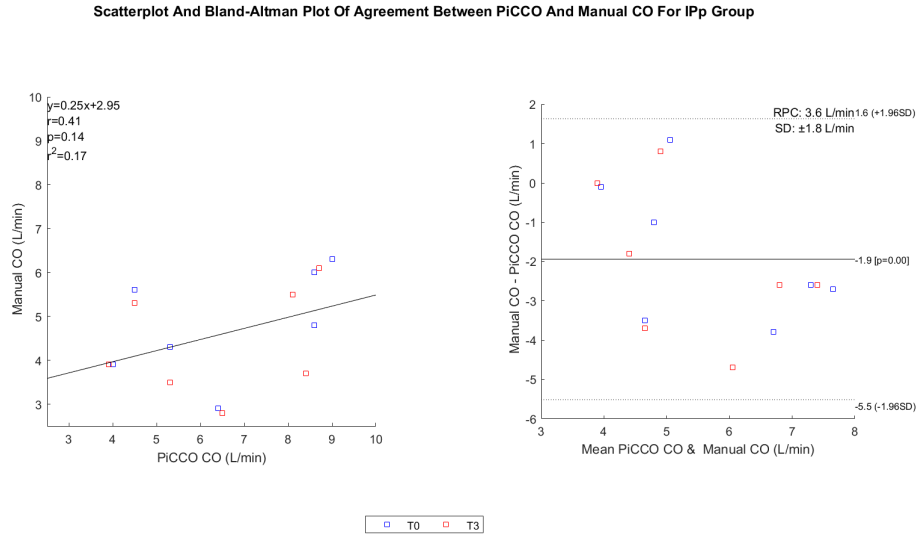

Figure 17: Scatter plot (left) and Bland-Altman plot of agreement (right) between PiCCO and manual CO for ICU patients with PiCCO (IPp)

4.6 Group Comparison

Both groups were compared for the group median cCO for the duration of the measurements. This is presented in Figure 18 and 19 for the static and dynamic measurements. As shown in Figure 18, the HVs have a median cCO between 2.6 and 3.2 l/min, with an IQR of 0.17 l/min, and has a sinusoidal pattern. The IPs have an median cCO between 2.8 and 3.3 l/min, with an IQR of 0.15 l/min, and a sinusoidal pattern. For the dynamic measurements, shown in Figure 19, the HVs have a median cCO between 2.4 and 3.0 l/min, with an IQR of 0.17 l/min. The IPs have a median cCO between 2.6 and 3.8 l/min, with an IQR of 0.29 l/min. No significant difference was found for the static cCO measurements between the HVs and the IP (p=0.294), nor for the dynamic measurements (p=0.518).

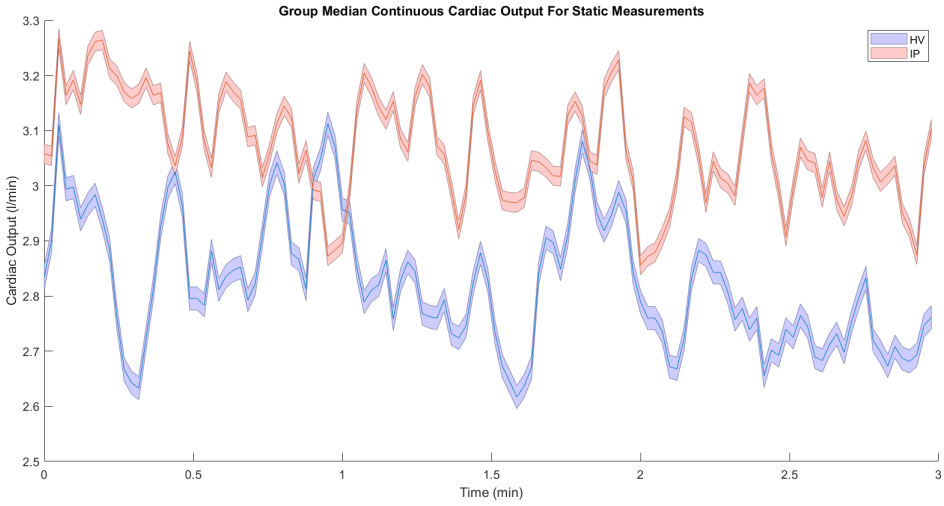

Figure 18: Group median cCO of HVs (blue) and IPs (red) for static measurements with the confidence intervals plotted along the lines

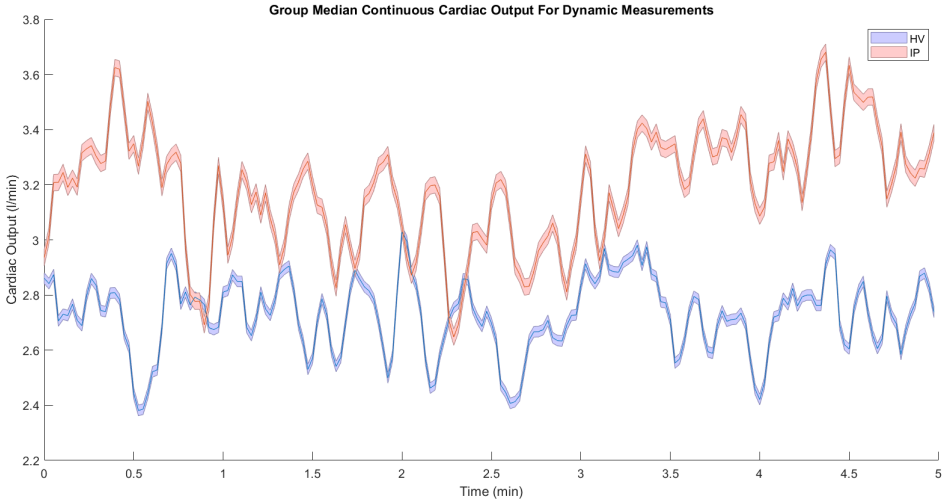

Figure 19: Group median cCO of HVs (blue) and IPs (red) for dynamic measurements with the confidence intervals plotted along the lines

5 Discussion

This research evaluated the feasibility and validity of cCO measurements in ICU patients. Moreover, differences in cCO measurements between HVs and IPs were investigated.

5.1 Interpretation of the Results

Feasibility of the static and dynamic measurements and analysis is as expected for both the HV and IP group. The HVs had a 100% feasibility and the IPs had an 88% feasibility for the static measurements. This feasibility is similar to earlier clinical studies with the ProbeFix that showed a feasibility of 80% [9] and 82% [30]. The 100% feasibility for HV is exceptionally high and might be explained by the fact that HVs are younger and have a lower BMI and therefore have better image quality [31]. For the dynamic measurements the feasibility was substantially lower, at 73% and 50%. The main reason for this was the loss of the DS signal due to small movements of the ProbeFix during the PLR test. Similar results were found in a study by Godfrey et al.[32], where 35% of subjects had a sub-optimal image quality during the PLR. Another reason for the lower feasibility, was the condition of the IPs, as 28% of patients' condition was not good enough to endure a PLR, thereby automatically failing the dynamic measurement. Finally, the feasibility of analysis was 100% for both the HV and IP group. Since every measurement that was successful could be analysed, resulting in 100% successful analysis. As for 12% of IPs no successful measurements could be accomplished, no analysis could be conducted as well. However, based on the definition for successful analysis, the absence of data did not affect these results.

The validity of the cCO measurements seems high, since the averages are within a realistic range. However, it is lower on average than expected. A normal CO measured with TTE for healthy subjects would be around 4.6 l/min (± 1.1 l/min) and for this research the average cCO was 2.8 l/min for the HVs [33]. The manual CO measurements had an average of 3.9 l/min and is therefore within a normal range. The lower average of the cCO measurements can be explained by the filtering of the DS. This filtering lowered the signal and eventually the CO. Another reason for the lower CO can be a low fluid balance among HVs, as during this research no fluid challenge is performed it is unclear whether or not the HVs are fluid responsive and when they last had some fluids. This could affect the CO on average, thereby lowering it, however this seems unlikely as HVs adequately regulate their own fluid intake. Similar results can be seen when examining the average cCO for patients. This is again within a realistic range as the average cCO for IPs was 3.4 l/min. However, it is still a bit lower than average, as normally patients have a CO around 4.0 l/min (± 0.9 l/min) [34]. This can again be explained by the filtering of the DS, which lowers the CO. The manual measured CO is a bit higher than the average at 4.9 l/min, but this is still within the SD. Finally, it is shown that there is no significant difference between the static and dynamic cCO measurements for both the HVs and the IPs. This outcome was not expected as the PLR, which was performed during the dynamic cCO measurements, is regarded as a method to assess fluid responsiveness by seeing an increase in CO when performing a PLR [35]. Therefore the lack of difference between static and dynamic measurements is most likely due to another reason. This difference is most likely caused by shifting of the ProbeFix during the PLR and thereby a loss of signal, which leads to a lower CO than that is expected. As it is stated that this is a common problem when performing PLR while using TTE [36].

A strong correlation (0.78 for HVs and 0.87 for IPs) between the manual and automatic CO calculations was found. This corresponds with other research, for example, Zhai et al.[37] also found a

correlation of 0.89 between automatic and manual calculated CO. Their higher correlation might be caused by their industrial developed AI to calculate the VTI and CO. A weak correlation was found between the PiCCO and automatic CO calculations (0.26) and between the PiCCO and manual CO calculations (0.41). Many studies found a better correlation between PiCCO and manual CO measurements. For example, Wurzer et al.[38] found a correlation of 0.73, Aslan et al.[39] found a correlation of 0.985, and Dai et al.[40] found a correlation of 0.8. This difference might be explained by the difference in measurement set-up. As the probe is first placed in the ProbeFix and then the manual CO is calculated, which could limit the degrees of motion. In most other studies the manual CO is calculated hands-free. Another explanation is the use of expert physicians to measure the manual CO. Most studies let an expert physician execute the manual CO, as in this study multiple calculations had to be made, researchers executed the manual CO measurements to minimize interobserver variability. Furthermore, our research contains only 8 IPp, so a factor that contributes to the weak correlation could be the small sample size. Another example is the research by Bobbia et al.[10], that found a correlation 0.83, between PiCCO and automatic CO, which is substantially higher than the findings in this research. An explanation might be the use of anesthetised piglets in the research by Bobbia et al., as this allowed them to better control their subjects during measurements. Another reason could be the filtering of the DS, which as stated before could lower the CO. A final reason might be that these values are not comparable with each other, as Wetterslev et al.[41] concluded after their systematic review, that the comparison between TTE en thermodilution techniques is difficult and the CO values are not interchangeable.

When comparing the measurements of the HVs with the IPs, the variation of cCO is lower for HVs (0.17 l/min for static and dynamic cCO measurements) than for IPs (0.15 l/min for static and 0.29 l/min for dynamic cCO measurements). This is expected, as patients are more hemodynamically unstable and therefore have more fluctuations in CO compared to healthy subjects [42, 43]. Furthermore, it is shown that the median cCO for HVs (2.8 l/min for static and 2.7 l/min for dynamic cCO measurements) is lower than the median cCO of patients (3.1 l/min for static and 3.2 l/min for dynamic cCO measurements). As stated before this is not expected, as HVs are known to have a higher CO (4.6 l/min) in comparison to IPs (4.0 l/min) [33, 34]. However, an argument could be the learning curve in the performance of the measurements for the researchers, as this method was first tested on the HVs and after that patient measurements started. Therefore creating better measurements for the IPs, which could lead to a higher CO. Despite the outcome, Figure 18 and 19 show the trend of the cCO over time, which is considered to be more important than the absolute values. As in critical care physicians tend to look more at trends than at absolute values, because they are a better indicator for patient deterioration [44].

Finally, when looking at the subject characteristics, it can be seen that the IP population is predominantly male, since men are more likely to be admitted to the ICU [45, 46]. Furthermore, there is a significant ($p<0.001$) age difference between the HVs (27 ±3 years) and IP (64 ±10 years), which corresponds to research as the average age for critically ill patients in the ICU is 64 years [47]. HVs were substantially younger because they were selected among a healthy, mostly junior, staff. Age can influence the CO, as a higher age is correlated to a lower CO [33]. However, in this study this was not seen. Furthermore, HVs had a normal BMI and ICU patients were overweight on average [48]. This can be expected as a large number of ICU patients are overweight [49]. This could affect the measurements as a higher BMI is associated with a lower echogenicity [31]. Lastly, it can be noted that most patients were admitted due to septic shock and are therefore monitored using a PiCCO catheter. This is primarily, because hemodynamic monitoring is vital for this category of

patients and therefore a PiCCO catheter is used as standard care. Also, this is often combined with the use of noradrenline and argipressine as medicinal treatment, therefore explaining why 66% of patients were receiving these medications. This might increase CO in comparison to IPp that do not receive these medication. [50, 51]

5.2 Strengths and Limitations

The main strength of this research was the use of a CO monitoring system that is both continuous and non-invasive. Many other studies are either focusing on continuous or non-invasive CO measurements [22, 52, 53, 54]. According to a recent review, methods that are considered continuous and non-invasive for hemodynamic monitoring are: pulse wave transit time, thoracic electrical bioimpedance/bioreactance, automated radial artery applanation tonometry and the vascular unloading method [55]. However, these methods still have multiple limitations. For the pulse wave transit time, bioimpedance and bioreactance many mathematical assumptions have to be made in order to calculate the CO. For the automated radial artery applanation tonometry and the vascular unloading method the computation of CO is based on pulse wave analysis, thereby indirectly calculating CO. The cCO method has neither of these limitations, as the CO is measured directly and no mathematical assumptions are made.

A second strength is the use of an automatic tool to calculate the CO for multiple minutes. Since TTE in its current clinical practise does not allow for the automatic calculation of the CO. Therefore, this study used and tested a tool that was developed specifically for this research. This tool was capable of calculating the CO for every subjects, since all analyses were successful. Only few other studies have used a tool like the one used in this study. As mentioned before an automatic VTI tool based on AI was used by Bobbia et al. [10], and by Zhai et al[37]. Furthermore, Mercadal et al.[56] also used an algorithm based on VTI in order to diagnose hemodynamic shock. Some companies have developed features like this tool into their ultrasound systems, however no clinical studies with these features have been conducted to our knowledge [57].

Another strength is the focus on feasibility of ICU patients, most research in hemodynamic monitoring studies focuses on the comparison of two techniques and not on the clinical feasibility in patients [38, 39, 40, 58, 59, 60, 61, 62]. Therefore, to our knowledge this research is the first to evaluate the feasibility of a continuous and non-invasive cardiac output monitoring system based on TTE. One example of another study that researched feasibility in a similar way to this research was performed by Kuster et al.[63] in which feasibility is also used as an outcome. However this study researched bioimpedance hemodynamic monitoring instead of TTE. Furthermore, this one of very few studies found when looking at the literature.

Fourthly, measurements were executed by only two researchers to decrease the inter-observer variability. This allowed for a small difference in outcomes. If both researchers were present, both had to agree on the tracing of the manual measurements to also minimize the intra-observer variability.

A final strength is the use of a two phase study design for feasibility in this research. This research first tested its method on HVs in order to determine feasibility. Therefore, ensuring that the cCO method was safe for and applicable to patients, limiting exposure to unnecessary burden. Only after this, patient testing was started as well as validation with a gold standard.

Several limitations to this study were identified. Firstly, the study was conducted on only 15 HVs and

18 patients due to time constraints, which is a small sample size. For a significant effect, sample size has to be increased with 46 patients, based on a sample size calculation. Furthermore, the two groups were not homogeneous with each other. Both groups were homogeneous on their own, but differed too much on age, gender and weight to make a valid comparison. This makes it difficult to compare the two groups regarding the cCO method, because differences in CO can be caused my multiple factors. Thereby limiting the ability of this study to make regards on this matter.

Secondly, this study uses the manual CO measurements as primary comparison for its new method. However, the gold standard in hemodynamic monitoring is considered to be PAC or sometimes PiCCO [64, 65, 66]. Manual CO was chosen as comparison as it could be used in both HVs and IPs and would not unnecessarily burden subjects. Patients with a PiCCO were included to allow for a secondary comparison, which was done for 8 IPp.

Thirdly, the ProbeFix itself had several limitations in its use. The main limitation was the angle the ProbeFix is able to make on the thorax because of its design. The three legs of the ProbeFix are equal in length and therefore the incline in angle can only be made from the ball joint. For some subjects, the maximal incline in the joint construction was not sufficient to get a solid A5C view and this angle had to be increased by lifting the two front legs of the ProbeFix. Furthermore, in some patients pressure marks were visible after the measurements. These pressure marks faded away quickly after the measurements were finished. Some subjects also experienced discomfort, when the ProbeFix was attached. This was similar to the research of Blans et al.[9] and therefore we limited the time of the study procedure to fifteen minutes to minimize potential discomfort or pressure marks.

5.3 Recommendations

Further research into the cCO method is needed. Firstly, the ProbeFix has to be further developed. As stated before, it was difficult in some patients to gain the right angle between the ProbeFix and the thorax and leaving the ProbeFix on for patients can cause discomfort, thereby impeding prolonged monitoring. Therefore, options have to be explored to make the ProbeFix more comfortable. Possible solutions would be to design extendable legs to be able to change the angle in multiple dimensions. For the pressure marks, the design of soft pillows on the legs would allow for more comfort. It is also possible that the ProbeFix is no longer needed in the future, as developments in ultrasound research focus on bio-adhesive ultrasound patches. Recent research showed that the patches are able to track changes in VTI and may even be more sensitive and specific for detecting decreased CO than standard vital signs in healthy volunteers [67].

Secondly, the algorithm needs to be further developed. First, the binarizing threshold needs to be further analysed. Now this threshold is set at 10, based on a few subjects from previous research. However, it could be that in a larger population this threshold changes. Second, the detection of the VTI could be further examined. This is now based on the derivative of the DS, however another method, for example a least squares method, could improve the signal and increasing the accuracy of the VTI detection, as this filters out more noise [68]. Third, the peak detection should be optimized, as this is now done apart from the heartbeat. In an optimal setting the peak would be detected based on the heartbeat, so no false artifacts can be detected as VTI nor will valid VTIs be skipped by the algorithm. Lastly, other parameters could be included into the algorithm. This study only focused on CO, however stroke volume variation is also often used as parameter for fluid responsiveness and could easily be integrated into the interface and algorithm. [69].

Thirdly, the cCO method needs to be adapted. The most important adaptation is to replace or cancel the dynamic measurements. As the PLR is not a sufficient method to detect changes in the CO. A better method would be the use of a microbolus of fluid (250 cc) and measure the CO during and after administration. By increasing the volume the CO should increase, and as subjects are not moved during the administration the feasibility for dynamic measurements could increase. Furthermore the use of a butterfly ultrasound device should be investigated. Right now the measurement set-up would claim one ultrasound system for a longer period of time, while most ICU wards have only one or two ultrasound systems. The use of a butterfly system is cheaper and therefore would make it easier for an ICU to invest in multiple butterfly systems. Furthermore, the butterfly system is smaller so it does not take up as much space as the larger ultrasound system. However, the butterfly system has a lower resolution, so it should be investigated if this still allows for a working algorithm .

Finally, based on a sample size calculation, an extra 46 patients have to be included, especially patients monitored with a PiCCO system. Since PiCCO is currently regarded as a gold standard of hemodynamic monitoring, the further inclusion of these patients would allow to better research the validity of the cCO method. Furthermore, more HVs should be included. We recommend to perform age- and gender-matching between the HVs and IPs to allow for a better comparison , which would again give more insight in the validity and the distinctiveness between HVs and IPs of the cCO method.

6 Conclusion

In conclusion, the cCO method is a feasible method for 88 percent of ICU patients and 100 percent of healthy volunteers. Measured values with the cCO method correspond strongly with manual measured CO and weakly correspond with PiCCO. Furthermore, no significant differences were found between healthy volunteers and ICU patients in this study. However, further research is needed to increase sample size and further develop the ProbeFix and the automatic calculation tool.

References

[1] Mainak Majumdar. “Haemodynamic Monitoring in the Intensive Care Unit”. In: *Intensive Care* (July 2017). DOI: 10.5772/INTECHOPEN.68591. URL: https://www.intechopen.com/chapters/55736.

[2] Manu L.N.G. Malbrain et al. “Hemodynamic monitoring in the critically ill: An overview of current cardiac output monitoring methods”. In: *F1000Research* 5.0 (2016), pp. 1–9. ISSN: 1759796X. DOI: 10.12688/f1000research.8991.1.

[3] Michael R. Pinsky. “Hemodynamic evaluation and monitoring in the ICU”. In: *Chest* 132.6 (2007), pp. 2020–2029. ISSN: 00123692. DOI: 10.1378/chest.07-0073. URL: http://dx.doi.org/10.1378/chest.07-0073.

[4] Sandra Funcke et al. “Practice of hemodynamic monitoring and management in German, Austrian, and Swiss intensive care units: the multicenter cross-sectional ICU-CardioMan Study”. In: *Annals of Intensive Care* 6 (2016), p. 49. DOI: 10.1186/s13613-016-0148-2.

[5] Philippe Vignon. “Continuous cardiac output assessment or serial echocardiography during septic shock resuscitation?” In: *Annals of Translational Medicine* 8.12 (June 2020), pp. 797–797. ISSN: 2305-5847. DOI: 10.21037/ATM.2020.04.11. URL: https://atm.amegroups.com/article/view/40996/html.

[6] Jordan King and David R. Lowery. “Physiology, Cardiac Output”. In: *StatPearls* (July 2021). URL: https://www.ncbi.nlm.nih.gov/books/NBK470455/.

[7] D C Evans et al. “COMPLICATIONS ASSOCIATED WITH PULMONARYA RTERY CATHETERS: ACOMPREHENSIVE CLINICAL REVIEW”. In: *REVIEW Scandinavian Journal of Surgery* 98 (2009), pp. 199–208.

[8] Mathieu Jozwiak et al. “What is the lowest change in cardiac output that transthoracic echocardiography can detect?” In: *Critical Care* 23.1 (2019), pp. 1–10. ISSN: 1466609X. DOI: 10.1186/s13054-019-2413-x.

[9] M. J. Blans, F. H. Bosch, and J. G. van der Hoeven. “The use of an external ultrasound fixator (Probefix) on intensive care patients: a feasibility study”. In: *Ultrasound Journal* 11.1 (2019). ISSN: 25248987. DOI: 10.1186/s13089-019-0140-9. URL: https://doi.org/10.1186/s13089-019-0140-9.

[10] Xavier Bobbia et al. “A new echocardiographic tool for cardiac output evaluation: An experimental study”. In: *Shock* 52.4 (2019), pp. 449–455. ISSN: 15400514. DOI: 10.1097/SHK.0000000000001273.

[11] Jason den Duijn. “Real-time automatic continuous cardiac output measurements using transthoracic echocardiography: a feasibility study”. In: february (2021).

[12] I. Visser. “Continuous and Automatic Monitoring of Cardiac Output by Transthoracic Echocardiography”. In: August (2021).

[13] C. Albers. “Continuous Monitoring of the Cardiac Output with the use of Transthoracic Echocardiography”. In: (2021).

[14] Jean Louis Vincent. “Understanding cardiac output”. In: *Critical Care* 12.4 (Aug. 2008), p. 174. ISSN: 13648535. DOI: 10.1186/CC6975. URL: /pmc/articles/PMC2575587/%20/pmc/articles/PMC2575587/?report=abstract%20https://www.ncbi.nlm.nih.gov/pmc/articles/PMC2575587/.

[15] Rob Oberman and Abhishek Bhardwaj. “Physiology, Cardiac”. In: *StatPearls* (July 2021). URL: https://www.ncbi.nlm.nih.gov/books/NBK526089/.

[16] Anthony V. Delicce and Amgad N. Makaryus. “Physiology, Frank Starling Law”. In: *StatPearls* (Feb. 2022). URL: https://www.ncbi.nlm.nih.gov/books/NBK470295/.

[17] Jean-Louis Vincent. “The pulmonary artery catheter”. In: *Journal of Clinical Monitoring and Computing* 2012.26 (2012), pp. 341–345. DOI: 10.1007/s10877-012-9389-2.

[18] Erwin E. Argueta and David Paniagua. “Thermodilution Cardiac Output: A Concept over 250 Years in the Making”. In: *Cardiology in Review* 27.3 (2019), pp. 138–144. ISSN: 15384683. DOI: 10.1097/CRD.0000000000000223.

[19] James Dean Sandham et al. *A Randomized, Controlled Trial of the Use of Pulmonary-Artery Catheters in High-Risk Surgical Patients*. Tech. rep. 2003. URL: www.nejm.org.

[20] Sheldon Magder. “Invasive hemodynamic monitoring”. In: *Critical Care Clinics* 31.1 (2015), pp. 67–87. ISSN: 15578232. DOI: 10.1016/j.ccc.2014.08.004. URL: http://dx.doi.org/10.1016/j.ccc.2014.08.004.

[21] Lisa Sangkum et al. “Minimally invasive or noninvasive cardiac output measurement: an update”. In: *Journal of anesthesia* 30.3 (June 2016), pp. 461–480. ISSN: 1438-8359. DOI: 10.1007/S00540-016-2154-9. URL: https://pubmed.ncbi.nlm.nih.gov/26961819/.

[22] E. Liton and M. Morgan. “The PiCCO monitor: A review”. In: *Anaesthesia and Intensive Care* 40.3 (May 2012), pp. 393–409. ISSN: 14480271. DOI: 10.1177/0310057x1204000304. URL: https://journals.sagepub.com/doi/10.1177/0310057X1204000304?url_ver=Z39.88-2003&rfr_id=ori%3Arid%3Acrossref.org&rfr_dat=cr_pub++0pubmed.

[23] Rebecca T Hahn FASE and Philippe Pibarot DVM FASE. “CORRESPONDENCE Accurate Measurement of Left Ventricular Outflow Tract Diameter: Comment on the Updated Recommendations for the Echocardiographic Assessment of Aortic Valve Stenosis”. In: *Journal of the American Society of Echocardiography* 30 (2017), pp. 1038–1041. DOI: 10.1016/j.echo.2017.06.002.

[24] Pablo Blanco. “Rationale for using the velocity–time integral and the minute distance for assessing the stroke volume and cardiac output in point-of-care settings”. In: *Ultrasound Journal* 12.1 (2020). ISSN: 25248987. DOI: 10.1186/s13089-020-00170-x. URL: https://doi.org/10.1186/s13089-020-00170-x.

[25] Lena M. Napolitano. “Sepsis 2018: Definitions and Guideline Changes”. In: *https://home.liebertpub.com/sur* 19.2 (Feb. 2018), pp. 117–125. ISSN: 15578674. DOI: 10.1089/SUR.2017.278. URL: https://www.liebertpub.com/doi/10.1089/sur.2017.278.

[26] Adrian Purcarea and Silvia Sovaila. “Sepsis, a 2020 review for the internist”. In: *Romanian journal of internal medicine = Revue roumaine de medecine interne* 58.3 (Sept. 2020), pp. 129–137. ISSN: 2501062X. DOI: 10.2478/RJIM-2020-0012.

[27] Michael D. Font, Braghadheeswar Thyagarajan, and Ashish K. Khanna. “Sepsis and Septic Shock – Basics of diagnosis, pathophysiology and clinical decision making”. In: *Medical Clinics of North America* 104.4 (July 2020), pp. 573–585. ISSN: 15579859. DOI: 10.1016/J.MCNA.2020.02.011.

[28] John Canny. “A Computational Approach to Edge Detection”. In: *IEEE TRANSACTIONS ON PATTERN ANALYSIS AND MACHINE INTELLIGENCE* 6 (1986).

[29] Patrick Schober and Lothar A. Schwarte. “Correlation coefficients: Appropriate use and interpretation”. In: *Anesthesia and Analgesia* 126.5 (May 2018), pp. 1763–1768. ISSN: 15267598. DOI: 10.1213/ANE.0000000000002864. URL: https://journals.lww.com/anesthesia-analgesia/Fulltext/2018/05000/Correlation_Coefficients__Appropriate_Use_and.50.aspx.

[30] O. A.E. Salden et al. “How i do it: Feasibility of a new ultrasound probe fixator to facilitate high quality stress echocardiography”. In: *Cardiovascular Ultrasound* 16.1 (2018), pp. 1–7. ISSN: 14767120. DOI: 10.1186/s12947-018-0124-0.

[31] Andrea Z. Pereira et al. “Muscle Echogenicity and Changes Related to Age and Body Mass Index”. In: *Journal of Parenteral and Enteral Nutrition* 45.7 (Sept. 2021), pp. 1591–1596. ISSN: 1941-2444. DOI: 10.1002/JPEN.2030. URL: https://onlinelibrary.wiley.com/doi/full/10.1002/jpen.2030%20https://onlinelibrary.wiley.com/doi/abs/10.1002/jpen.2030%20https://aspenjournals.onlinelibrary.wiley.com/doi/10.1002/jpen.2030.

[32] G. E.P. Godfrey, S. W. Dubrey, and J. M. Handy. “A prospective observational study of stroke volume responsiveness to a passive leg raise manoeuvre in healthy non-starved volunteers as assessed by transthoracic echocardiography”. In: *Anaesthesia* 69.4 (Apr. 2014), pp. 306–313. ISSN: 1365-2044. DOI: 10.1111/ANAE.12560. URL: https://onlinelibrary.wiley.com/doi/full/10.1111/anae.12560%20https://onlinelibrary.wiley.com/doi/abs/10.1111/anae.12560%20https://associationofanaesthetists-publications.onlinelibrary.wiley.com/doi/10.1111/anae.12560.

[33] Hena N Patel et al. “Normal Values of Cardiac Output and Stroke Volume According to Measurement Technique, Age, Sex, and Ethnicity: Results of the World Alliance of Societies of Echocardiography Study HHS Public Access”. In: *J Am Soc Echocardiogr* 34.10 (2021), pp. 1077–1085. DOI: 10.1016/j.echo.2021.05.012. URL: https://doi.org/10.1016/j.echo.2021.05.012..

[34] F. Franchi et al. “Echocardiography and pulse contour analysis to assess cardiac output in trauma patients”. In: *Minerva anestesiologica* 79.2 (Feb. 2013), pp. 137–146. ISSN: 1827-1596. URL: https://pubmed.ncbi.nlm.nih.gov/23032925/.

[35] Xavier Monnet, Paul Marik, and Jean Louis Teboul. “Passive leg raising for predicting fluid responsiveness: a systematic review and meta-analysis”. In: *Intensive Care Medicine 2016 42:12* 42.12 (Jan. 2016), pp. 1935–1947. ISSN: 1432-1238. DOI: 10.1007/S00134-015-4134-1. URL: https://link.springer.com/article/10.1007/s00134-015-4134-1.

[36] Wojciech Mielnicki, Agnieszka Dyla, and Tomasz Zawada. “Utility of transthoracic echocardiography (TTE) in assessing fluid responsiveness in critically ill patients - A challenge for the bedside sonographer”. In: *Medical Ultrasonography* 18.4 (2016), pp. 508–514. ISSN: 20668643. DOI: 10.11152/mu-880.

[37] Shanshan Zhai et al. “Artificial intelligence (AI) versus expert: A comparison of left ventricular outflow tract velocity time integral (LVOT-VTI) assessment between ICU doctors and an AI tool”. In: *Journal of Applied Clinical Medical Physics* (July 2022), e13724. ISSN: 1526-9914. DOI: 10.1002/ACM2.13724. URL: https://onlinelibrary.wiley.com/doi/full/10.1002/acm2.13724%20https://onlinelibrary.wiley.com/doi/abs/10.1002/acm2.13724%20https://aapm.onlinelibrary.wiley.com/doi/10.1002/acm2.13724.

[38] Paul Wurzer et al. “Transpulmonary Thermodilution Versus Transthoracic Echocardiography for Cardiac Output Measurements in Severely Burned Children”. In: *Shock* 46.3 (2016), pp. 249–253. ISSN: 15400514. DOI: 10.1097/SHK.0000000000000627.

[39] Nagehan Aslan et al. “Comparison of cardiac output and cardiac index values measured by critical care echocardiography with the values measured by pulse index continuous cardiac output (PiCCO) in the pediatric intensive care unit:a preliminary study”. In: *Italian journal of pediatrics* 46.1 (Apr. 2020). ISSN: 1824-7288. DOI: 10.1186/S13052-020-0803-Y. URL: https://pubmed.ncbi.nlm.nih.gov/32299455/.

[40] Rongqin Dai et al. “[Clinical value of point of care ultrasound on cardiac output and volume responsiveness in patients with septic shock]”. In: *Zhonghua wei zhong bing ji jiu yi xue* 33.12 (Dec. 2021), pp. 1479–1483. ISSN: 2095-4352. DOI: 10.3760/CMA.J.CN121430-20210610-00800. URL: https://pubmed.ncbi.nlm.nih.gov/35131016/.

[41] Mik Wetterslev et al. “Systematic review of cardiac output measurements by echocardiography vs. thermodilution: the techniques are not interchangeable”. In: *Intensive Care Medicine* 42.8 (2016), pp. 1223–1233. ISSN: 14321238. DOI: 10.1007/s00134-016-4258-y.

[42] Maja Elstad et al. “Low-frequency fluctuations in heart rate, cardiac output and mean arterial pressure in humans: What are the physiological relationships?” In: *Journal of Hypertension* 29.7 (2011), pp. 1327–1336. ISSN: 14735598. DOI: 10.1097/HJH.0b013e328347a17a.

[43] Chung Chi Huang et al. “Spontaneous variability of cardiac output in ventilated critically ill patients”. In: *Critical Care Medicine* 28.4 (2000), pp. 941–946. ISSN: 00903493. DOI: 10.1097/00003246-200004000-00005.

[44] Matthew M. Churpek, Richa Adhikari, and Dana P. Edelson. “The value of vital sign trends for detecting clinical deterioration on the wards”. In: *Resuscitation* 102 (May 2016), pp. 1–5. ISSN: 18731570. DOI: 10.1016/J.RESUSCITATION.2016.02.005. URL: https://www.researchgate.net/publication/295093733_The_value_of_vital_sign_trends_for_detecting_clinical_deterioration_on_the_wards.

[45] Peter Dodek et al. “More men than women are admitted to 9 intensive care units in British Columbia”. In: *Journal of Critical Care* 24.4 (Dec. 2009), pp. 1–630. ISSN: 0883-9441. DOI: 10.1016/J.JCRC.2009.02.010.

[46] Atanas Todorov et al. “Gender differences in the provision of intensive care: a Bayesian approach”. In: *Intensive Care Medicine* 47 (2021), pp. 577–587. DOI: 10.1007/s00134-021-06393-3. URL: https://doi.org/10.1007/s00134-021-06393-3.

[47] Allan Garland et al. “Epidemiology of critically ill patients in intensive care units: A population-based observational study”. In: *Critical Care* 17.5 (Sept. 2013), pp. 1–7. ISSN: 13648535. DOI: 10.1186/CC13026/FIGURES/3. URL: https://ccforum.biomedcentral.com/articles/10.1186/cc13026.

[48] Miet Schetz et al. “Obesity in the critically ill: a narrative review”. In: *Intensive care medicine* 45.6 (June 2019), pp. 757–769. ISSN: 1432-1238. DOI: 10.1007/S00134-019-05594-1. URL: https://pubmed.ncbi.nlm.nih.gov/30888440/.

[49] Henry Oliveros and Eduardo Villamor. “Obesity and mortality in critically ill adults: A systematic review and meta-analysis”. In: *Obesity* 16.3 (2008), pp. 515–521. ISSN: 19307381. DOI: 10.1038/oby.2007.102.

[50] Zhongheng Zhang, Hongying Ni, and Zhixian Qian. “Effectiveness of treatment based on PiCCO parameters in critically ill patients with septic shock and/or acute respiratory distress syndrome: a randomized controlled trial”. In: *Intensive Care Medicine* 41.3 (Mar. 2015), pp. 444–451. ISSN: 14321238. DOI: 10.1007/S00134-014-3638-4/FIGURES/2. URL: https://link.springer.com/article/10.1007/s00134-014-3638-4.

[51] Swathikan Chidambaram et al. “Vasopressin vs noradrenaline: Have we found the perfect recipe to improve outcome in septic shock?” In: *Journal of Critical Care* 49 (Feb. 2019), pp. 99–104. ISSN: 0883-9441. DOI: 10.1016/J.JCRC.2018.10.029.

[52] Richard A. Bernstein et al. “Effect of Long-term Continuous Cardiac Monitoring vs Usual Care on Detection of Atrial Fibrillation in Patients With Stroke Attributed to Large- or Small-Vessel Disease: The STROKE-AF Randomized Clinical Trial”. In: *JAMA* 325.21 (June 2021), pp. 2169–2177. ISSN: 1538-3598. DOI: 10.1001/JAMA.2021.6470. URL: https://pubmed.ncbi.nlm.nih.gov/34061145/.

[53] Takeshi Suzuki et al. “Cardiac output and stroke volume variation measured by the pulse wave transit time method: a comparison with an arterial pressure-based cardiac output system”. In: *Journal of Clinical Monitoring and Computing* 33.3 (June 2019), pp. 385–392. ISSN: 15732614. DOI: 10.1007/S10877-018-0171-Y.

[54] Guijun Zhu et al. “Accuracy assessment of noninvasive cardiac output monitoring in the hemodynamic monitoring in critically ill patients”. In: *Annals of Cardiothoracic Surgery* 9.5 (2020), pp. 3506–3512. ISSN: 23041021. DOI: 10.21037/apm-20-1731.

[55] Bernd Saugel, Maurizio Cecconi, and Ludhmila Abrahao Hajjar. “Noninvasive Cardiac Output Monitoring in Cardiothoracic Surgery Patients: Available Methods and Future Directions”. In: *Journal of Cardiothoracic and Vascular Anesthesia* 33.6 (2019), pp. 1742–1752. ISSN: 15328422. DOI: 10.1053/j.jvca.2018.06.012. URL: https://doi.org/10.1053/j.jvca.2018.06.012.

[56] J. Mercadal et al. “A simple algorithm for differential diagnosis in hemodynamic shock based on left ventricle outflow tract velocity–time integral measurement: a case series”. In: *The Ultrasound Journal* 14.1 (Aug. 2022), pp. 1–11. ISSN: 25248987. DOI: 10.1186/S13089-022-00286-2/FIGURES/4. URL: https://theultrasoundjournal.springeropen.com/articles/10.1186/s13089-022-00286-2.

[57] Carmit Shiran and Igor Barjaktarevic. *Venue™ Family Auto Tool for Measuring VTI*. 2021. URL: https://www.pocushub.net/data/venue-family_auto-vti_whitepaper_pocus__glob_jb02194xx.pdf.

[58] M. Biais et al. “Ability of esCCO to track changes in cardiac output”. In: *British Journal of Anaesthesia* 115.3 (2015), pp. 403–410. ISSN: 14716771. DOI: 10.1093/bja/aev219.

[59] Ulrike Ehlers et al. “Continuous Estimation of Cardiac Output in Critical Care: A Noninvasive Method Based on Pulse Wave Transit Time Compared with Transpulmonary Thermodilution”. In: *Critical Care Research and Practice* 2020 (2020). ISSN: 20901313. DOI: 10.1155/2020/8956372.

[60] Marc Feissel et al. “Pulse wave transit time measurements of cardiac output in septic shock patients: A comparison of the estimated continuous cardiac output system with transthoracic echocardiography”. In: *PLoS ONE* 10.6 (2015), pp. 1–13. ISSN: 19326203. DOI: 10.1371/journal.pone.0130489. URL: http://dx.doi.org/10.1371/journal.pone.0130489.

[61] Pablo Mercado et al. “Transthoracic echocardiography: An accurate and precise method for estimating cardiac output in the critically ill patient”. In: *Critical Care* 21.1 (2017), pp. 1–8. ISSN: 1466609X. DOI: 10.1186/s13054-017-1737-7.

[62] A. S. McLean et al. “Estimation of cardiac output by noninvasive echocardiographic techniques in the critically ill subject”. In: *Anaesthesia and Intensive Care* 25.3 (1997), pp. 250–254. ISSN: 0310057X. DOI: 10.1177/0310057x9702500307.

[63] Matthias Kuster et al. “Non-invasive cardiac output monitoring device “ICON” in trauma patients: a feasibility study”. In: *European Journal of Trauma and Emergency Surgery* 45.6 (2019), pp. 1069–1076. ISSN: 16153146. DOI: 10.1007/s00068-018-0984-x. URL: http://dx.doi.org/10.1007/s00068-018-0984-x.

[64] Chen Li et al. “The effects of hemodynamic monitoring using the PiCCO system on critically ill patients”. In: *Am J Transl Res* 13.9 (2021). URL: www.ajtr.org.

[65] Jacob Pugsley and Adam B. Lerner. “Cardiac output monitoring: Is there a gold standard and how do the newer technologies compare?” In: *Seminars in Cardiothoracic and Vascular Anesthesia* 14.4 (Dec. 2010), pp. 274–282. ISSN: 10892532. DOI: 10.1177/1089253210386386. URL: https://journals.sagepub.com/doi/10.1177/1089253210386386?url_ver=Z39.88-2003&rfr_id=ori%3Arid%3Acrossref.org&rfr_dat=cr_pub++0pubmed.

[66] Sherrie Smartt. “The pulmonary artery catheter: Gold standard or redundant relic”. In: *Journal of Perianesthesia Nursing* 20.6 (Dec. 2005), pp. 373–379. ISSN: 10899472. DOI: 10.1016/j.jopan.2005.09.006. URL: http://www.jopan.org/article/S1089947205002819/fulltext%20http://www.jopan.org/article/S1089947205002819/abstract%20https://www.jopan.org/article/S1089-9472(05)00281-9/abstract.

[67] Jon-Émile S Kenny et al. “The Feasibility of a Novel Index From a Wireless Doppler Ultrasound Patch to Detect Decreasing Cardiac Output in Healthy Volunteers”. In: *Military Medicine* 186.1 (2021). DOI: 10.1093/milmed/usaa248.

[68] Michael Schmid, David Rath, and Ulrike Diebold. “Why and How SavitzkyGolay Filters Should Be Replaced”. In: *Cite This: ACS Meas. Sci. Au* 2022 (2022), pp. 185–196. DOI: 10.1021/acsmeasuresciau.1c00054. URL: https://doi.org/10.1021/acsmeasuresciau.1c00054.

[69] Zhongheng Zhang et al. “Accuracy of stroke volume variation in predicting fluid responsiveness: a systematic review and meta-analysis”. In: *Japanese Society of Anesthesiologists* (2011). DOI: 10.1007/s00540-011-1217-1.

Appendix A: Matlab scripts

Step 1: Reading data

```
%% READING DATA
clear all
close all
clc

% Choose dicom file
x='IM_0017';
%%
filename = ['E:\Data\ICPp\ICPp_08\',x];
%pathway

info = dicominfo(filename);                                    % Read metadata

TTE_video = dicomread(filename);                               % Read image data

%% Input arguments
d = 2.1;                                                       % Diameter of LVOT [cm]
Ylim = 140;                                                   % Y-axis limit of TTE ...
    [cm/s], has to be read from the DICOM image manually.

%% Show image or video

if ndims(TTE_video)==4
    implay(TTE_video)
elseif ndims(TTE_video)==3
    imshow(TTE_video)
end
```

Step 2: Image to signal

```
%% FROM IMAGE TO SIGNAL

% Load settings
FileSize = info.FileSize;
Frames = info.NumberOfFrames;
HR = info.HeartRate;                                            % HR from video

%% Select DS signal

% Step 1: Select last frame
TTE = TTE_video(:,:,:,23);                                     % Select first full VTI frame
fontsize = 16;                                                  % Fontsize in figures
%figure(1), imshow(TTE), title('Step 1: Select last frame','Fontsize',fontsize)

% Step 2: Crop TTE
[redObjectsMask,rows,cols] = BaselineDetection(TTE);
UB = min(rows);                                                 % Find upper boundary,
LoB = length(TTE(:,1,1,1));                                     % Choose lower boundary ...
    manually
RB = find(redObjectsMask(UB,:),1,'last');                       % Find right boundary
LB=34;
```

```
DS = TTE(UB:end,LB:RB,:,end);                                    % Crop TTE

% Step 3: Find frame of interest
RUC = squeeze(TTE_video(UB,RB,:,:));                            % Select upper right ...
    corner of DS for all frames.
[redObjectsMask2,rows,cols] = BaselineDetection(RUC);

FrameOfInterest = find(redObjectsMask2,1,'first');          % Select first frame ...
    displaying red at corner.
Loops=Frames/FrameOfInterest;
nloops=floor(Loops);

%% Image to Signal per loop

 for i=1:nloops

   %figure(2), subplot(2,2,1), imshow(DS), title('Step 2: Crop image','Fontsize',fontsize)

    DopplerSpectrum = TTE_video(UB:LoB,LB:RB,:,FrameOfInterest*i);

    %subplot(2,2,2), imshow(DopplerSpectrum), title('Step 3: Find frame of ...
        interest','Fontsize',fontsize)

    % Step 4: Binarize image
    [BinaryDopplerSpectrum] = Binarize(DopplerSpectrum);

    %subplot(2,2,3), imshow(BinaryDopplerSpectrum), title('Step 4: Binarize ...
        image','Fontsize',fontsize)

%     Step 5: Find edges
    [EdgesDopplerSpectrum] = FindEdges(BinaryDopplerSpectrum);

    %subplot(2,2,4), imshow(EdgesDopplerSpectrum), title('Step 5: Find and connect ...
        edges','Fontsize',fontsize)

    % Step 6: image to signal
    Width = size(EdgesDopplerSpectrum,2);                       % Number of pixels in ...
        x-direction
    v_unscaled = zeros(1,Width);                                % Preallocate vector
    for n = 1:Width
        dummy = find(EdgesDopplerSpectrum(:,n),1,'first');      % Find first white ...
            pixel moving downwards.
        if ¬ isempty(dummy)                                     % If not empty
            v_unscaled(n) = dummy;
        end
    end

%     figure(3), imshow(DopplerSpectrum), hold on,
%     plot(v_unscaled,'Color','white','Linewidth',3), title('Step 6: Image to ...
    signal','Fontsize',fontsize),
%     legend('Doppler spectrum signal','Location','southeast','Color',[0.7 0.7 ...
    0.7],'EdgeColor','w', 'TextColor','w','Fontsize',fontsize)
```

```
    % Preprocess signal

    % Scale time-axis.
    CineRate = info.CineRate;                                   % Frames per second [1/s]
    RecordingTime = FrameOfInterest/CineRate;                   % Recording time [s]
    Ts = RecordingTime/length(v_unscaled);                      % Sampling period [s]
    t = Ts:Ts:RecordingTime;                                    % Create time vector [Sec]
    Endtime=t(1,end);

    % Scale velocity-axis
    PixelSize = Ylim/size(EdgesDopplerSpectrum,1);              % Pixel size ...
        [(cm/s)/pixel]
    v_scaled = PixelSize * v_unscaled;                          % Scaled velocity [cm/s]

    % Smooth signal using a Savitzky-Golay filter using 25-sample frames and first ...
        order polynomials.
    v_smooth(i,:) = sgolayfilt(v_scaled,1,25);
end
```

Step 3: Combining the segments

```
    %% Combining v_smooth

nloops=length(v_smooth(:,1));
v_total=v_smooth(1,:);
for i=1:nloops
    v_total=[v_total(1,:) v_smooth(i,:)];
end

t_total = Ts:Ts:(Ts*length(v_smooth));

% plot(t_total,v_smooth)
% xlabel('Time(sec)')
%xlim([0 10])

%% Compose struct

Struct.name=x;
Struct.v_total=v_total;
Struct.Info=info;
Struct.dLVOT=d;
Struct.t_total=t_total;
Struct.Ts=Ts;

savename=['Struct_ICPp_08_Stat','.mat'];
save(savename,'Struct') %save signal as struct
```

Step 4: VTI estimation and CO calculation

```
    %% Sliding window with continuous CO monitor

clear all
close all

% Loading struct
load('Struct_ICPnp_01_Stat.mat')

%% Personal Settings

v_total=Struct.v_total;
info=Struct.Info;
HR_loaded=Struct.Info.HeartRate;
d=Struct.dLVOT;
fontsize = 10;

% Signal processing
Ts =  Struct.Ts;                                          % Sampling period
t_total = Ts:Ts:(Ts*length(v_total));                     % Create time vector [Sec]

% Mean line
meanline = mean(v_total);

%% excessive data removal

v_remove=find(v_total<0);
v_total(v_remove)=[];
t_total(v_remove)=[];

figure()
plot(t_total,v_total)

promptMessage = sprintf('Are extreme outliers present?');
titleBarCaption = 'Yes or No';
numberOfUsers = 1;
buttonSelections = zeros(1, numberOfUsers); % Preallocate.
for userNumber = 1 : numberOfUsers
  button = questdlg(promptMessage, titleBarCaption, 'Yes', 'No', 'Yes');
  if strcmpi(button, 'Yes')
    buttonSelections(userNumber) = 1;
  else
    buttonSelections(userNumber) = -1;
  end
  if buttonSelections(userNumber) == 1
    prompt = "What is the cut-off value? ";
    cut_off_value = input(prompt);
    v_remove=find(v_total>cut_off_value);
    v_total(v_remove)=[];
    t_total(v_remove)=[];
  else
     continue
  end
end
```

```
%% Finding corrupted data and removing it
u=v_total';
t=t_total'; % column vector of time

N=length(t);

plot(t_total,v_total)
title('Select point above which data is corrupted','FontSize',fontsize)
[corrupt_x,corrupt_y] = ginput(1);
ns=find(u>corrupt_y); % say corrupted at these ns

if ¬isempty(ns)
    k=1;
    x=1;

    for i=1:length(ns)-1
        noise(x,k)=ns(i,1);
        x=x+1;

        if ns(i+1,1)-ns(i,1)≠1
            k=k+1;
            x=1;
        end
    end

    noise(noise == 0) = NaN;

    urecov=u; % the recovered u is u ...

    for b=1:length(noise(1,:))
        ns2=noise(:,b);
        ns2=(ns2(¬isnan(ns2)));

        if ns2(1,1)≤20
            ns1(:,1)=(ns2(1,1):1:ns2(end,1)+20);
        else
            ns1(:,1)=(ns2(1,1)-20:1:ns2(end,1)+20);
        end
        M=length(ns1); % number of corrupted u's
        plot(t,u)
        hold on
        plot(t(ns1),u(ns1),'*r')

        B=[1 -3 3 -1]; % 3rd order derivative
        bd=length(B)-1; % degree = 3
        x=filter(B,1,u);
        W=zeros(N,M);
        for k=1:M
            W(ns1(k)+[0:bd]',k)=B';
        end
        c=W\x;
        urecov(ns1)=u(ns1)-c; % modify corrupted data
        clearvars ns1 ns2
    end
```

```
    figure;
    subplot(2,1,1)
    plot(t,u,'Color','w','LineWidth',1,'HandleVisibility','off')
    axis tight, set(gca,'XLimSpec','Tight','Color','k','Fontsize',fontsize)
    xlim([5 20])
    ylim([0 120])
    ylabel('v (cm/s)','FontSize',fontsize)
    xlabel('Time (s)','FontSize',fontsize)

    title('Original Data','FontSize',fontsize)
    subplot(2,1,2)
    plot(t,urecov,'Color','w','LineWidth',1,'HandleVisibility','off')
    set(gca,'XLimSpec','Tight','Color','k','Fontsize',fontsize)
    title('Recovered Data','FontSize',fontsize)
    xlim([5 20])
    ylim([0 120])
    ylabel('v (cm/s)','FontSize',fontsize)
    xlabel('Time (s)','FontSize',fontsize)

    v_total=urecov;
end

%% FindPeaks to detect the start and end of systole

% Detect times of maximal velocity.
MPH = 0.75*max(v_total);                                    % Minimal Peak Height ...
    [cm/s]
MPD= 0.5*(60/HR_loaded)/Ts;                                     % Minimal Peak ...
    Distance
[max_pks,max_locs] = findpeaks(v_total,'MinPeakHeight',MPH);%,'MinPeakDistance',MPD);

% Detect start and end of systole.
dv = diff(v_total);                                         % Derivate: ...
    acceleration [cm/s^2]

start = zeros(1,length(max_pks)); stop = zeros(1,length(max_pks)); % Preallocate vector
start_pos = zeros(1,length(max_pks)); stop_pos = zeros(1,length(max_pks)); % ...
    Preallocate vector

% Find points where the derivative crossing the zero-line
dummies=zerocrossings(dv);

% Allocate start, peak and stop for each heartbeat
for n = 1:length(max_pks)

    if n==1
        start(n)=1;
        stop_pos(n)=find(dummies>max_locs(n)+1 & v_total(dummies)<meanline,1,'first');
        stop(n)=dummies(stop_pos(n));

    elseif n == length(max_pks)

        start_pos(n)=find(dummies<max_locs(n)-1,1,'last');
        start(n)=dummies(start_pos(n));

        if dummies(end)≥max_locs(n)
            stop_pos(n)=find(dummies>max_locs(n)+1,1,'first');
            stop(n)=dummies(stop_pos(n));
```

```
        else
            stop(n)=length(v_total)-1;
        end

    else

        start_pos(n)=find(dummies<max_locs(n)-1 & v_total(dummies)<meanline,1,'last');
        start(n)=dummies(start_pos(n));
        stop_pos(n)=find(dummies>max_locs(n)+1,1,'first');
        stop(n)=dummies(stop_pos(n));

    end
    heartbeat(n,1)=start(n);
    heartbeat(n,2)=max_locs(n);
    heartbeat(n,3)=stop(n);

end

%% Detect length of heartbeat (useful for window selection)

for i=1:length(heartbeat)
    One_heartbeat(i,1)=start(i);
    if i == length(heartbeat)
        One_heartbeat(i,2)=length(v_total);
    else
        One_heartbeat(i,2)=start(i+1)-1;
    end
end

%% Sliding window across the signal in main graph

numberofheartbeats=2;                               % Number of additional heartbeats ...
    for the mean calculation
N_windows=length(One_heartbeat)-numberofheartbeats; % Number of windows

% Open main figure
f1=figure(1);
sgtitle('CONTINUOUS CALCULATION OF CARDIAC OUTPUT ICPnp-1','FontSize',20)
set(f1, 'units','normalized','outerposition',[0 0 1 1]);

ax=subplot(4,2,2);
ht=text(0.5,0.5,'-','FontSize',30);
title('Cardiac Output Value (L/min)','FontSize',fontsize)
set(ax, 'visible', 'off')
set(findall(ax, 'type', 'text'), 'visible', 'on')

ax=subplot(4,2,6);
hr=text(0.5,0.5,'-','FontSize',30);
title('Stroke Volume Variation (%)','FontSize',fontsize)
set(ax, 'visible', 'off')
set(findall(ax, 'type', 'text'), 'visible', 'on')
```

```
% Calculating the Cardiac Output per window
for i = 1:N_windows

    figure(f1),subplot(4,2,1), ...
        plot(t_total,v_total,'Color','w','LineWidth',1,'HandleVisibility','off'),
    ylabel('v (cm/s)','Fontsize',fontsize), title('Complete Doppler ...
        Signal','Fontsize',fontsize),
    axis tight, set(gca,'XLimSpec','Tight','Color','k','Fontsize',fontsize)

    % Select window
    boundary_R(i) = One_heartbeat(i+numberofheartbeats,2)+50;
    if i == N_windows
        boundary_R(i) = One_heartbeat(i+numberofheartbeats,2);
        boundary_L(i) = One_heartbeat(i,1)-50;
    elseif i == 1
        boundary_L(i) = One_heartbeat(i,1)+1;
    else
        boundary_L(i) = One_heartbeat(i,1)-50;                              % Left ...
            window boundary
    end

    boundary(i)=boundary_R(i)-boundary_L(i);
    t = t_total(boundary_L(i):boundary_R(i));                           % Time vector ...
        of window
    v_window = v_total(boundary_L(i):boundary_R(i));                    % Velocity ...
        vector of window
    subplot(4,2,1), hold on,
    rectangle('Position',[boundary_L(i)*Ts 0 boundary(i)*Ts ...
        max(v_total)],'Edgecolor','#D95319','Linewidth',4)
    hold off

    % Moving the start point to create better results
    %percent=round(0.2*(mean(abs(heartbeat(i,1)-heartbeat(i,3)))));

    start_window = zeros(1,numberofheartbeats+1); stop_window = ...
        zeros(1,numberofheartbeats+1); % Preallocate vector

    % Load start, peak and stop location
    for k=1:numberofheartbeats+1
        k=k-1;
        start_window(k+1)=heartbeat(i+k,1);%+percent;
        max_locs_window(k+1)=heartbeat(i+k,2);
        stop_window(k+1)=heartbeat(i+k,3);
    end

    dv=diff(v_window);
    dv_total=diff(v_total);
```

```
% Start plotting
subplot(4,2,3), plot(t,v_window,'Color','w','Linewidth',2,'HandleVisibility','off'),
hold on, scatter(t_total(max_locs_window),v_total(max_locs_window),100,'filled',
'MarkerFaceColor','#EDB120'),
hold on,
ylabel('v (cm/s)','Fontsize',fontsize), title('Window','Fontsize',fontsize),
axis tight, set(gca,'XLimSpec','Tight','Color','k','Fontsize',fontsize)
legend({'Max'},'Location','eastoutside','Color','k','EdgeColor','w','TextColor','w',
'Fontsize',12);
hold off

subplot(4,2,5), ...
    plot(t(1,1:end-1),dv,'Color','w','Linewidth',2,'HandleVisibility','off'),hold on,
ylabel('a (cm/s^2)','Fontsize',fontsize),title('Derivative','Fontsize',fontsize),
scatter(t_total(start_window),dv_total(start_window),100,'filled','c',
'MarkerFaceColor','#A2142F'),
scatter(t_total(max_locs_window),dv_total(max_locs_window),100,'c','filled',
'MarkerFaceColor','#EDB120'),
scatter(t_total(stop_window),dv_total(stop_window),100,'c','filled',
'MarkerFaceColor','#D95319'),

hold on,
legend({'Start','Max','End'},'Location','eastoutside','Color','k','EdgeColor','w',
'TextColor','w','Fontsize',12);
axis tight,   ylim([-4 4]), ...
    set(gca,'XLimSpec','Tight','Color','k','Fontsize',fontsize)
hold off

subplot(4,2,7), ...
    plot(t,v_window,'Color','w','LineWidth',1,'HandleVisibility','off'),hold on,
scatter(t_total(start_window),v_total(start_window),100,'filled','c',
'MarkerFaceColor','#A2142F'),
scatter(t_total(max_locs_window),v_total(max_locs_window),100,'filled',
'MarkerFaceColor','#EDB120'),
scatter(t_total(stop_window),v_total(stop_window),100,'c','filled',
'MarkerFaceColor','#D95319'),
for n = 1:length(max_locs_window)
    area(t_total(start_window(n):stop_window(n)),
    v_total(start_window(n):stop_window(n)),
    'Facecolor','w','FaceAlpha',.8,'Edgecolor','w','Linewidth',1)
end
hold on
xlabel('Time (s)','Fontsize',fontsize), ylabel('v (cm/s)','Fontsize',fontsize),
title('VTI Estimation','Fontsize',fontsize), ...
    set(gca,'XLimSpec','Tight','Color','k','Fontsize',fontsize),
legend({'Start','Max','End','VTI'},'Location','eastoutside',...
    'Color','k','EdgeColor','w','TextColor','w','Fontsize',12);
hold off

%   FOR CHANGING HEARTBEAT ( only possible when timevector problem is solved
%   HR1=mean(diff(max_locs_window));
%   HR2=HR1*Ts;
%   HR_average=60/HR2;
HR_average=HR_loaded;
```

```
    % Calculate Velocity Time Integral
    VTI = zeros(1,length(max_locs_window));                                    % ...
        Preallocate vector
    for n = 1:length(max_locs_window)
        T = t_total(start_window(n):stop_window(n)); ...
                                                    % Point spacing
        V = v_total(start_window(n):stop_window(n)); ...
                                                % Velocity
        VTI(i,n) = floor(trapz(T,V));                                          % ...
            Integrate V with respect to T.
    end
    VTI_average(i) = round(mean(VTI(i,:)),1);

    % Calculate Cardiac Output
    CSA = pi*(d/2)^2;                                          % Cross-sectional ...
        area of the LVOT [cm^2]
    CSA = round (CSA,2);
    SV(i) = round(CSA * VTI_average(i));                                % Stroke ...
        volume [mL]
    CO(i) = round((HR_average * SV(i))/1000,1);                           % Cardiac ...
        output [L/min]
    HR(i) = HR_average;

    subplot(4,2,2)
    strCO=num2str(CO(i));
    ht.String = strCO;

    subplot(4,2,[4 6]),plot(CO,'-o','Color','r','MarkerSize',2,'MarkerFaceColor','red'),
    xlabel('Window'), ylabel('CO (L/min)','Fontsize',fontsize), title('Cardiac ...
        Output','Fontsize',fontsize),
    axis tight, set(gca,'XLimSpec','Tight','Color','k','Fontsize',fontsize), grid on
    ylim([0 8]),xlim([0 N_windows])

%% Display mean, min and max
CO_mean=mean(CO)
CO_min=min(CO)
CO_max=max(CO)
CO_variation = CO_max - CO_min
```

Appendix B: Data per subject

	CO_mean_stat	CO_max_stat	CO_min_stat	CO_mean_dyn	CO_max_dyn	CO_min_dyn
HV_01	3,7	5,2	2,9	3,7	5,9	2,8
HV_02	2,8	3,5	2	-	-	-
HV_03	2,7	3,4	1,8	2,8	4,9	1,6
HV_04	3,5	4,9	2,5	-	-	-
HV_05	2,1	2,5	1,7	2,2	3,8	1,5
HV_06	3,1	3,7	2	2,7	5,2	1,5
HV_07	2,6	5	1,3	2,4	3,8	1,7
HV_08	1,7	6	1,1	1,5	2,3	1,1
HV_09	3,1	4,2	2,2	3,7	4,5	2,4
HV_10	3,5	5,6	2,3	3,1	4,5	2
HV_11	3	4,1	2,1	2.8	3,4	1,9
HV_12	1,7	2,4	1,2	-	-	-
HV_13	1,6	1,9	0,9	-	-	-
HV_14	2,6	3,8	1,9	2,2	3	1,7
HV_15	3,7	4,5	2,8	4,1	5,7	2,8

Table 4: cCO data per HV

	CO_man_t0	CO_cont_t0	CO_diff_t0	CO_man_t3	CO_cont_t3	CO_diff_t3
HV_01	4,2	3,6	0,6	3,9	3,9	0
HV_02	4,5	3,1	1,4	3,7	3,1	0,6
HV_03	3,4	3	0,4	3,8	2,6	1,2
HV_04	4,6	3,5	1,1	4	3,3	0,7
HV_05	3,1	2,5	0,6	3,4	2,1	1,3
HV_06	4,2	3,2	1	3,7	3,4	0,3
HV_07	4,1	2,3	1,8	4,2	2,4	1,8
HV_08	4,1	3,4	0,7	2,6	1,5	1,1
HV_09	4,5	3,1	1,4	5	3,5	1,5
HV_10	4,6	4	0,6	5,2	3,8	1,4
HV_11	4,2	3	1,2	4,2	3	1,2
HV_12	4,1	2,4	1,7	4	2,3	1,7
HV_13	3,1	1,8	1,3	3,4	1,6	1,8
HV_14	3,4	2,4	1	3,6	2,6	1
HV_15	5,4	4,4	1	5,9	4,1	1,8

Table 5: Difference between manual and automatic CO per HV

	CO_mean_stat	CO_max_stat	CO_min_stat	CO_mean_dyn	CO_max_dyn	CO_min_dyn
ICPnp_01	2,2	2,8	1,2	2,3	3,1	1,7
ICPnp_02	8,2	9,9	5,1	8,1	9,8	5,6
ICPnp_03	-	-	-	-	-	-
ICPnp_04	3,2	4,8	1,9	-	-	-
ICPnp_05	3,5	4,1	2,6	3,4	4,8	2,1
ICPnp_06	3,6	4,2	2,3	3,6	5,2	2,4
ICPnp_07	2,8	4,7	1,8	-	-	-
ICPnp_08	2,8	4	1,2	3,1	5,7	1,9
ICPnp_09	3	6,1	1,9	-	-	-
ICPnp_10	3,1	4,8	1,6	3,2	5,2	2
ICPp_01	1,8	2,4	1,3	2	2,7	1,4
ICPp_02	5,3	9,9	3,3	-	-	-
ICPp_03	1,5	2,2	0,7	1,5	2,1	0,7
ICPp_04	-	-	-	-	-	-
ICPp_05	3	4,6	1,8	-	-	-
ICPp_06	2,7	4,3	1,8	-	-	-
ICPp_07	4,6	8,7	3,3	4,2	6,7	2,2
ICPp_08	3,1	4,2	2	-	-	-

Table 6: cCO data per IP

	CO_man_t0	CO_cont_t0	CO_t0_diff	CO_man_t3	CO_cont_t3	CO_t3_diff
ICPnp_01	4,3	2,1	2,2	4,1	2,3	1,8
ICPnp_02	8,8	8	0,8	8,7	8,5	0,2
ICPnp_03	-	-	-	-	-	-
ICPnp_04	5,5	3,6	1,9	5,2	3,6	1,6
ICPnp_05	4,7	3,7	1	4,1	3,7	0,4
ICPnp_06	5	3,3	1,7	5,1	3,8	1,3
ICPnp_07	5,4	4,7	0,7	4,5	2,8	1,7
ICPnp_08	4,5	2,5	2	4,9	3,7	1,2
ICPnp_09	4,2	3,1	1,1	4,5	2,8	1,7
ICPnp_10	4,3	2,9	1,4	3,4	2,2	1,2
ICPp_01	2,9	1,6	1,3	2,8	1,8	1
ICPp_02	6,3	4,2	2,1	6,1	5	1,1
ICPp_03	4,8	1,6	3,2	3,7	1,4	2,3
ICPp_04	-	-	-	-	-	-
ICPp_05	6	2,7	3,3	5,5	2,7	2,8
ICPp_06	4,3	4,3	0	3,5	2,6	0,9
ICPp_07	5,6	4,6	1	5,3	4,4	0,9
ICPp_08	3,9	3,1	0,8	3,9	3,2	0,7

Table 7: Difference between manual and automatic CO per IP

Appendix C: Statistical output

Statistical Output Subject Characteristics Table 1

Tests of Normality

	Kolmogorov-Smirnov[a]			Shapiro-Wilk		
	Statistic	df	Sig.	Statistic	df	Sig.
Gender_HV_num	,352	13	<,001	,646	13	<,001
Gender_ICP_num	,431	13	<,001	,592	13	<,001
Age_HV	,265	13	,013	,867	13	,047
Age_ICP	,202	13	,150	,860	13	,038
Length_ICP	,199	13	,165	,919	13	,246
Length_HV	,179	13	,200*	,910	13	,185
weigth_HV	,178	13	,200*	,920	13	,251
Weigth_ICP	,245	13	,032	,747	13	,002
BMI_ICP	,227	13	,065	,841	13	,022
BMI_HV	,174	13	,200*	,929	13	,333
BSA_ICP	,212	13	,114	,851	13	,029
BSA_HV	,144	13	,200*	,926	13	,306
LVOTd_ICP	,415	13	<,001	,650	13	<,001
LVOTd_HV	,505	13	<,001	,446	13	<,001
MedUse_HV	.	13	.	.	13	.
MedUse_ICP	,470	13	<,001	,533	13	<,001

*. This is a lower bound of the true significance.

a. Lilliefors Significance Correction

Figure 20: Normality test subject characteristics Table 1

T-Test

Independent Samples Test

		Levene's Test for Equality of Variances		t-test for Equality of Means							
						Significance		Mean Difference	Std. Error Difference	95% Confidence Interval of the Difference	
		F	Sig.	t	df	One-Sided p	Two-Sided p			Lower	Upper
Length_all	Equal variances assumed	,142	,709	-,117	31	,454	,908	-,00411	,03519	-,07588	,06766
	Equal variances not assumed			-,115	27,822	,455	,909	-,00411	,03569	-,07725	,06903

Figure 21: Independent samples test of subject characteristics Table 1 for variable length

Mann-Whitney Test

Test Statistics[a]

	Gender_all	Age_all	Weigth_all	BMI_all	BSA_all	LVOTd_all	MedUse_all
Mann-Whitney U	100,500	7,500	60,000	60,500	71,500	102,500	45,000
Wilcoxon W	220,500	127,500	180,000	180,500	191,500	222,500	165,000
Z	-1,473	-4,621	-2,720	-2,694	-2,296	-,947	-3,904
Asymp. Sig. (2-tailed)	,141	<,001	,007	,007	,022	,344	<,001
Exact Sig. [2*(1-tailed Sig.)]	,215[b]	<,001[b]	,006[b]	,006[b]	,020[b]	,495[b]	<,001[b]

a. Grouping Variable: groups

b. Not corrected for ties.

Figure 22: Mann-Whitney U test for other subject characteristics of Table 1

Statistical Output Subject Characteristics Table 2

Tests of Normality

	Kolmogorov-Smirnov[a]			Shapiro-Wilk		
	Statistic	df	Sig.	Statistic	df	Sig.
Gender_IPp_num	,407	6	,002	,640	6	,001
Gender_IPnp_num	,407	6	,002	,640	6	,001
Age_IPnp	,244	6	,200*	,820	6	,088
Age_IPp	,326	6	,045	,808	6	,069
Length_IPp	,266	6	,200*	,849	6	,156
Length_IPnp	,182	6	,200*	,934	6	,609
weigth_IPnp	,285	6	,139	,757	6	,023
Weigth_IPp	,346	6	,023	,730	6	,012
BMI_IPp	,271	6	,193	,840	6	,129
BMI_IPnp	,251	6	,200*	,882	6	,277
BSA_IPp	,267	6	,200*	,851	6	,161
BSA_IPnp	,313	6	,067	,775	6	,035
LVOTd_IPp	,407	6	,002	,640	6	,001
LVOTd_IPnp	,392	6	,004	,701	6	,006
MedUse_IPp	,492	6	<,001	,496	6	<,001
MedUse_IPnp	,407	6	,002	,640	6	,001

*. This is a lower bound of the true significance.

a. Lilliefors Significance Correction

Figure 23: Normality test subject characteristics Table 2

T-Test

Independent Samples Test

		Levene's Test for Equality of Variances		t-test for Equality of Means							
						Significance				95% Confidence Interval of the Difference	
		F	Sig.	t	df	One-Sided p	Two-Sided p	Mean Difference	Std. Error Difference	Lower	Upper
Age_all	Equal variances assumed	,312	,584	-,008	16	,497	,994	-,050	6,386	-13,587	13,487
	Equal variances not assumed			-,008	15,721	,497	,994	-,050	6,122	-13,046	12,946
length_all	Equal variances assumed	4,671	,046	-,252	16	,402	,804	-,01150	,04557	-,10809	,08509
	Equal variances not assumed			-,239	11,086	,408	,815	-,01150	,04807	-,11720	,09420
BMI_all	Equal variances assumed	5,979	,026	,335	16	,371	,742	,9709	2,9014	-5,1798	7,1215
	Equal variances not assumed			,314	10,289	,380	,760	,9709	3,0933	-5,8953	7,8371

Figure 24: Independent samples test of normally distributed subject characteristics of Table 2

Mann-Whitney Test

Test Statistics[a]

	Gender_all	Weigth_all	BSA_All	LVOTd_all	MedUse_all
Mann-Whitney U	33,000	34,000	40,000	24,500	25,000
Wilcoxon W	69,000	70,000	95,000	60,500	80,000
Z	-,800	-,536	,000	-,489	-1,630
Asymp. Sig. (2-tailed)	,423	,592	1,000	,625	,103
Exact Sig. [2*(1-tailed Sig.)]	,573[b]	,633[b]	1,000[b]	,694[b]	,203[b]

a. Grouping Variable: Groups

b. Not corrected for ties.

Figure 25: Mann-Whitney U test for non-parametric subject characteristics of Table 2

Statistical Output of cCO measurements

Tests of Normality

	Kolmogorov-Smirnov[a]			Shapiro-Wilk		
	Statistic	df	Sig.	Statistic	df	Sig.
mean_CO_HV_stat	,145	15	,200*	,919	15	,188
mean_CO_HV_dyn	,155	11	,200*	,965	11	,835
mean_CO_ICP_stat	,262	16	,004	,797	16	,003
mean_CO_ICP_dyn	,255	9	,095	,806	9	,024

*. This is a lower bound of the true significance.

a. Lilliefors Significance Correction

Figure 26: Normality test cCO data

T-Test

Paired Samples Test

		Paired Differences					t	df	Significance	
					95% Confidence Interval of the Difference					
		Mean	Std. Deviation	Std. Error Mean	Lower	Upper			One-Sided p	Two-Sided p
Pair 1	mean_CO_HV_stat - mean_CO_HV_dyn	,0545	,3328	,1003	-,1690	,2781	,544	10	,299	,599

Figure 27: Paired samples test between static and dynamic cCO measurements for HV group

Nonparametric Tests

Hypothesis Test Summary

	Null Hypothesis	Test	Sig.[a,b]	Decision
1	The median of differences between mean_CO_ICP_stat and mean_CO_ICP_dyn equals 0.	Related-Samples Wilcoxon Signed Rank Test	,731	Retain the null hypothesis.

a. The significance level is ,050.

b. Asymptotic significance is displayed.

Related-Samples Wilcoxon Signed Rank Test Summary

Total N	9
Test Statistic	16,000
Standard Error	5,809
Standardized Test Statistic	,344
Asymptotic Sig.(2-sided test)	,731

Figure 28: Wilcoxon signed rank test between static and dynamic cCO measurements for IP group

Mann-Whitney Test

Ranks

	VAR00001	N	Mean Rank	Sum of Ranks
mean_CO_Stat	,00	15	14,23	213,50
	1,00	16	17,66	282,50
	Total	31		

Test Statistics[a]

	mean_CO_Stat
Mann-Whitney U	93,500
Wilcoxon W	213,500
Z	-1,050
Asymp. Sig. (2-tailed)	,294
Exact Sig. [2*(1-tailed Sig.)]	,299[b]

a. Grouping Variable: VAR00001

b. Not corrected for ties.

Figure 29: Mann-Whitney U test between HV and IP for static cCO measurements

Mann-Whitney Test

Ranks

	Groups	N	Mean Rank	Sum of Ranks
Mean_CO_dyn_ALL	0	11	9,73	107,00
	1	9	11,44	103,00
	Total	20		

Test Statistics[a]

	Mean_CO_dyn_ALL
Mann-Whitney U	41,000
Wilcoxon W	107,000
Z	-,647
Asymp. Sig. (2-tailed)	,518
Exact Sig. [2*(1-tailed Sig.)]	,552[b]

a. Grouping Variable: Groups

b. Not corrected for ties.

Figure 30: Mann-Whitney U test between HV and IP for dynamic cCO measurements